NASA TECHNICAL NOTE

NASA TN D-7990

NASA TN D-7990

APOLLO EXPERIENCE REPORT - GUIDANCE AND CONTROL SYSTEMS: LUNAR MODULE ABORT GUIDANCE SYSTEM

Pat M. Kurten

Lyndon B. Johnson Space Center
Houston, Texas 77058

NATIONAL AERONAUTICS AND SPACE ADMINISTRATION • WASHINGTON, D. C. • JULY 1975

1. Report No.	2. Government Accession No.	3. Recipient's Catalog No.
NASA TN D-7990		

4. Title and Subtitle	5. Report Date
APOLLO EXPERIENCE REPORT GUIDANCE AND CONTROL SYSTEMS: LUNAR MODULE ABORT GUIDANCE SYSTEM	July 1975
	6. Performing Organization Code JSC-08589
7. Author(s) Pat M. Kurten	8. Performing Organization Report No. JSC S-424
9. Performing Organization Name and Address Lyndon B. Johnson Space Center Houston, Texas 77058	10. Work Unit No. 976-10-41-01-72
	11. Contract or Grant No.
12. Sponsoring Agency Name and Address National Aeronautics and Space Administration Washington, D.C. 20546	13. Type of Report and Period Covered Technical Note
	14. Sponsoring Agency Code

15. Supplementary Notes

16. Abstract

The history of a unique development program that produced an operational fixed guidance system of inertial quality is presented in this report. Each phase of development, beginning with requirement definition and concluding with qualification and testing, is addressed, and developmental problems are emphasized. Software generation and mission operations are described, and specifications for the inertial reference unit are included, as are flight performance results. Significant program observations are noted.

17. Key Words (Suggested by Author(s))

- Display Devices
- Hardware
- Mission Trajectory
- Short Circuit
- Monte Carlo Method
- Software (Computers)
- Lunar Landing
- Accelerometers

18. Distribution Statement

STAR Subject Category:
12 (Astronautics, General)

19. Security Classif. (of this report)	20. Security Classif. (of this page)	21. No. of Pages	22. Price*
Unclassified	Unclassified	73	$4.25

*For sale by the National Technical Information Service, Springfield, Virginia 22151

CONTENTS

TABLES

FIGURES

APOLLO EXPERIENCE REPORT

GUIDANCE AND CONTROL SYSTEMS:

LUNAR MODULE ABORT GUIDANCE SYSTEM

By Pat M. Kurten
Lyndon B. Johnson Space Center

SUMMARY

With respect to the lunar module abort guidance system, the Apollo Program experience included the full range of program development from requirements through design, development, and production and culminated with successful flight. As a result of preliminary lunar-abort concepts, a strapped-down inertial-sensor package for attitude reference and an open-loop programer were selected to provide ascent steering for lunar-orbit insertion. A clear pericynthion orbit could be obtained by postinsertion burns, and rendezvous was to be accomplished by means of external information. A program redefinition in 1964 added the requirement for a clear pericynthion orbit from the initial abort burn and the requirement for a rendezvous within the lunar module fuel budget without information from sources outside the lunar module. The required accuracy of the strapped-down package was therefore increased, and a general-purpose digital computer containing 4096 words of memory replaced the open-loop programer. A display and keyboard device was added for crew communications with the computer.

INTRODUCTION

The lunar module (LM) abort guidance system (AGS) represents the first operational usage of a strapped-down guidance system. The AGS was designed and developed specifically for application in the Apollo LM. The AGS is composed of a strapped-down (or fixed) inertial-sensor package, the abort sensor assembly (ASA); a general-purpose digital computer with specialized input/output, the abort electronics assembly (AEA); and a display and keyboard device for crew communication with the computer, the data entry and display assembly (DEDA). The AGS forms the digital portion of a hybrid digital/analog guidance and control system and is configured to provide automatic control for mission abort resulting from a primary guidance system (PGS) malfunction.

The AGS was supplied by the LM prime contractor under NASA cognizance at the NASA Lyndon B. Johnson Space Center (JSC) (formerly the Manned Spacecraft Center (MSC)). The system responsibility of the AGS was subcontracted. The ASA was

further subcontracted by the subcontractor to the ASA vendor. The software for the AEA was contracted by MSC directly to the subcontractor.

As an aid to the reader, where necessary the original units of measure have been converted to the equivalent value in the Système International d'Unités (SI). The SI units are written first, and the original units are written parenthetically thereafter.

ACRONYMS

ACE	acceptance checkout equipment
AEA	abort electronics assembly
AGS	abort guidance system
ASA	abort sensor assembly
BPA	Bethpage, New York
C&W	caution and warning
CARR	customer acceptance readiness review
CDH	constant differential height
CDU	coupling data unit
CES	control electronics system
CM	command module
CSI	coelliptic sequence initiate
CSM	command and service module
DEDA	data entry and display assembly
DMCP	design mission computer program
DR	design report
DTO	detailed test objective
DVT	design verification test
EL	electroluminescent
EMI	electromagnetic interference

EPC	Earth prelaunch calibration
FACI	first article configuration inspection
FEB	functional electronic block
FMES	full mission engineering simulation
FRR	flight readiness review
FS	flight simulator
GSE	ground-support equipment
HSSC	Hamilton Standard System Center
HVSIR	H-vector spin input rectification
IA	input axis
ICS	interpretive computer simulation
IFC	in-flight calibration
JSC	Lyndon B. Johnson Space Center
KSC	John F. Kennedy Space Center
LM	lunar module
LOS	line of sight
LSC	lunar surface calibration
MSC	Manned Spacecraft Center
MSOB	Manned Spacecraft Operations Building
OA	output axis
PERT	program evaluation reporting technique
PIC	preinstallation calibration
PGNCS	primary guidance, navigation, and control system
PGS	primary guidance system
PTSA	pulse torquing servoamplifier

RCS reaction control system

RTV room-temperature vulcanizing

SA spin axis

SI Système International d'Unités

TPI terminal phase initiate

DISCUSSION

Preliminary LM Abort Concepts

The preliminary LM abort concepts included definition of early requirements and preliminary mechanization.

Early requirements. - The AGS was developed to provide the capability for safe crew abort from the powered descent, lunar surface, and powered ascent phases of the lunar mission. During these critical mission phases, information cannot be obtained from the command module (CM) or Earth that will ensure crew safety after failure of the primary guidance, navigation, and control system (PGNCS). The ground rules that defined the preliminary concepts of the AGS hardware are as follows.

1. Crew safety is primary. This ground rule implies that mission abort will be initiated if one additional failure will cause loss of crewmen. On a vehicle having a PGS and an AGS, failure of either will result in an abort because one additional guidance failure will not allow safe rendezvous with the CM.

2. Abort capability must exist at all times in case of a single PGS failure. The capability to initiate an abort must be independent of the LM phasing with the command and service module (CSM). The AGS must be capable of coping with initial conditions at any instant during powered descent and ascent. The capability of launching from the lunar surface at any time must exist.

3. The AGS must have independent operation. The AGS should be designed to operate without dependence on the PGS during critical mission phases.

4. The AGS should be simple. The system should be able to abort to a clear pericynthion of 12 192 meters (40 000 feet) at initial injection or at a later correction if no additional hardware is required for the later correction. The CSM, through a communication link to the LM, will be used to provide the LM with information for performing midcourse corrections. Rendezvous from abort should be completed within the LM fuel capacity.

5. An all-attitude inertial reference should be provided in the AGS. This requirement was established to ensure a reference if the three-gimbaled PGS should encounter gimbal lock.

6. The AGS need not be designed to complete the lunar landing mission. This rule does not imply that there is not some point in time when the LM will land with a PGS failure.

7. The AGS should have the capability of using both the ascent and descent stages of the LM. This provision was made to use the fuel in the descent stage as well as in the ascent stage after an abort.

Modification of the preceding ground rules was considered to enable the use of a simpler attitude reference system, such as a pair of gyros having two degrees of freedom. The requirement for the LM to complete the rendezvous with onboard fuel would be modified to have the LM establish itself in a clear pericynthion orbit in the plane of the CSM orbit. The requirement for the LM to abort to a clear orbit would be modified to put the LM on an intercept path with the CSM. These modifications to the ground rules were examined and discarded, primarily because of the increased fuel usage with an inaccurate system, the increased burden on CSM activity, and the unsafe trajectories involved.

Preliminary mechanization. - The ground rule requiring LM abort to a clear pericynthion orbit and requiring onboard fuel to complete rendezvous made an inertial-quality attitude reference system a necessity. A four-gimbaled inertial platform and a strapped-down attitude reference were considered. The strapped-down inertial reference was selected. The development risks associated with a strapped-down system were outweighed by the mechanical simplicity, the inherent ruggedness, the ease of maintenance, and the potential of the strapped-down system as a lightweight, reliable system for the LM abort mission and for future space applications. At the time of evaluation, the weight of the strapped-down sensors (gyros and accelerometers) was estimated at 7 kilograms (15 pounds); the associated electronics were estimated at 10.9 kilograms (24 pounds).

An open-loop programer was selected to provide the ascent steering necessary for a clear lunar orbit. A programer with an estimated weight of 9 kilograms (20 pounds) was the least complex, proven device for accomplishing this function because AGS navigation was not required. The programer provided a vehicle pitch sequence based on time of abort and stored constants and produced a thrust cutoff signal based on the velocity output of an accelerometer mounted along the vehicle thrust axis. A compensation scheme was incorporated into the program to correct for tolerances inherent in vehicle propulsion. The compensation scheme compared velocity readings from the thrust axis accelerometer taken at specified time intervals with nominal velocity values for adjusting pitch attitude and velocity at cutoff. Two accelerometers mounted normal to the thrust axis provided attitude biasing in correction of vehicle thrust misalinement. (The system outputs were attitude error signals for controlling vehicle attitude, total-attitude signals for display, and an engine-off signal.) The programer was envisioned as a 2048-word computer having a fixed memory. A control panel weighing approximately 4.5 kilograms (10 pounds) completed the preliminary mechanization concept.

Program Redefinition

The following program redefinition was made concerning AGS requirements and mechanization.

Requirements. - In the fall of 1964, a series of LM program redefinition meetings was held biweekly to reconfigure the LM guidance and control systems, including the AGS. Several changes were made to the ground rules covering the existing conceptual design.

1. The AGS should be capable of performing rendezvous with the CM within the LM fuel budget without information from sources outside the LM.

2. The AGS should provide information for monitoring the PGS.

3. The AGS should be capable of providing LM abort to the CSM from any phase of the LM mission.

4. The AGS should be capable of inserting the LM into a clear pericynthion orbit of 9144 meters (30 000 feet) above the Moon. This requirement originated because the height of some of the lunar mountains was determined to be 8839 meters (29 000 feet), although the mountains were not on the lunar equator, the landing site, or the lunar-orbit location. This requirement also necessitated clear pericynthion on the first abort burn and thus increased the accuracy requirement of the inertial reference.

5. The AGS attitude reference should be maintained at 25 deg/sec angular rotation. This requirement was established because of the vehicle rates necessary for proper vehicle response to manual commands during the final phase of lunar landing.

Mechanization. - Revision of the ground rules resulted in discarding the open-loop programer concept because of inflexibility and incapability. A general-purpose computer containing 4096 words was selected to replace the programer.

Navigation capability was added to the software, and an explicit guidance law was selected to perform the rendezvous. A hard-line interface between the rendezvous radar and the computer was added for navigation updates. This interface was later changed to a manual interface because of a mechanization problem.

A connection between the PGS digital telemetry downlink and the AGS computer was added to obtain state vector initialization information for navigation; this addition augmented the existing alinement interface for attitude reference alinement to the PGS. A digital telemetry downlink was added from the AEA. Added to the existing total-attitude and attitude error displays were computer interfaces for displaying altitude, altitude rate, and lateral velocity for monitoring the PGS.

The AGS therefore became a full guidance system. After alinement from the PGS with attitude information and after initialization with LM and CSM position, velocity, and epoch time data, the AGS continuously computes LM attitude, LM and CSM position

and velocity, and abort trajectories for predetermined orbital insertion conditions or for orbital transfers to the CSM. The assemblies comprising the AGS are shown in figure 1.

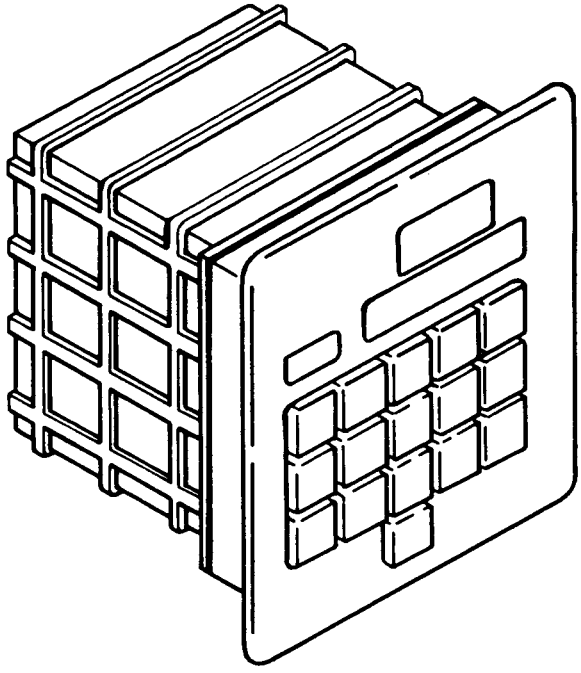

(a) Data entry and display assembly.

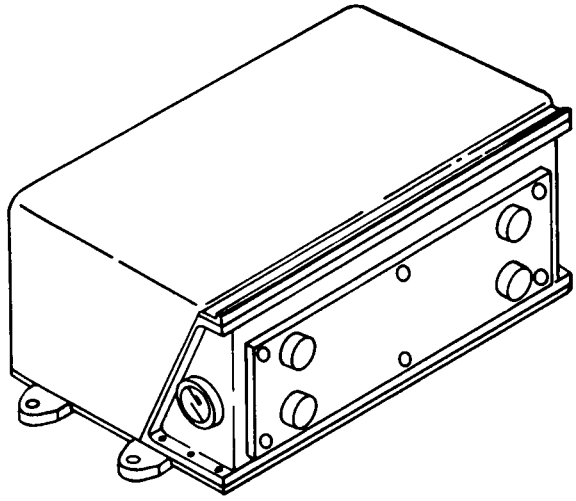

(b) Abort sensor assembly.

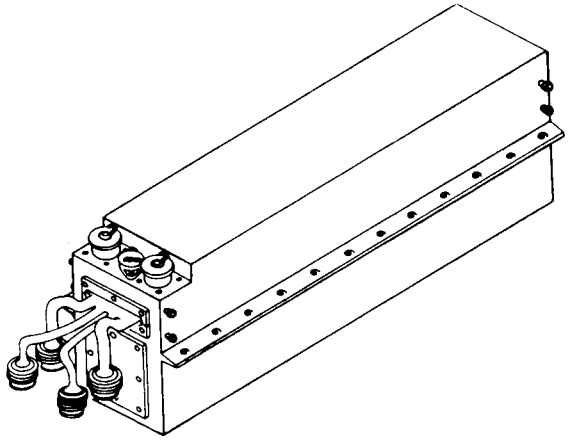

(c) Abort electronics assembly.

Figure 1. - Abort guidance system components.

System Description

The devices comprising the AGS are the AEA, the DEDA, and the ASA.

Abort electronics assembly. - The AEA is a general-purpose, high-speed digital computer that performs strapped-down attitude reference computations and navigation and guidance functions required to steer the LM to rendezvous. The AEA consists of a core memory, control and arithmetic logic, input/output circuitry, and a power supply. The assembly weighs 14.8 kilograms (32.7 pounds) and has dimensions of 60.32 by 20 by 13.33 centimeters (23.75 by 8 by 5.25 inches). The AEA (1) processes input information from the ASA, the DEDA, and the PGS; (2) performs attitude reference alinement and state vector initialization; (3) calibrates in-flight, lunar surface, and accelerometer biases; (4) performs self-tests; (5) maintains attitude reference; (6) performs navigation computations; (7) selects mode;

(8) performs guidance computations; (9) outputs steering and engine commands; (10) processes telemetry; and (11) displays outputs for in-flight monitoring.

Half of the 4096 words of memory in the AEA are hardwired and half are erasable. Fifty-three escape points exist throughout the wired memory so that corrections can be made, as required, in softwired memory. The memory uses 0.0008-meter (30 mil) ferrite cores wired in 64 by 64 planes, one plane for each word bit. The word length is 18 bits. Data words consist of a sign and 17 magnitude bits. Instructions consist of 18 bits that contain the order code and a single operand address.

The memory is a coincident current, parallel, random-access core memory with a cycle time of 5 microseconds. The functions located in the fixed memory are those that require the fastest computation or those that are mission independent (or both types); that is, direction cosine and tangent routines. Values that might feasibly vary from mission to mission, such as the guidance equations and the radar filter, are located in the erasable memory. Computer computations are done in 20-millisecond, 40-millisecond, and 2-second cycles. The direction cosine matrix is updated 50 times per second; the attitude error and engine commands are computed during the 40-millisecond cycle; and navigation and guidance are computed during the 2-second cycle.

The computer uses a fractional two's complement parallel arithmetic section. The computer add time is 10 microseconds; the multiply time, 70 microseconds. The AEA executes 27 basic instructions. The clock frequency is 1.024 megahertz. A 50-word digital telemetry downlink is outputted from the AEA once per second.

Integrated circuits, thin film networks, and multilayer circuit boards are used extensively to minimize size and weight. All subassemblies except the power supply are packaged in groups of multilayer boards interconnected by a wiring matrix. Split-pin wire wrapping is used to connect the multilayer boards to the matrix. The matrix carries all signal lines between the core memory, the arithmetic and control logic, and the input/output circuitry. Power is distributed by laminated bus bars encapsulated in the wiring matrix. The power supply modules are of cordwood construction. The sideplates of the AEA are attached to cold rails on which the AEA is mounted in the LM aft equipment bay. The AEA dissipates 81 watts of power.

Data entry and display assembly. - The DEDA is used to control AGS modes of operation, to insert data in the AEA manually, and to command the contents of accessible AEA memory to be displayed on numeric readouts. Manual control is accomplished by depression of pushbuttons on the DEDA panel in the required sequence. The DEDA, AEA, and ASA external configurations are shown in figure 1.

The DEDA consists of two main assemblies: a control panel housing the electroluminescent (EL) numeric display and the data-entry pushbuttons, and a logic enclosure housing the drive circuits, the input/output circuits, the power conditioning circuits, and the logic circuits. The logic enclosure is a hermetically sealed assembly housing nine multilayer circuit boards. The DEDA circuitry is composed of flatpacks and thin film networks. The DEDA has access to 452 of the 4096 memory locations in the AEA. Manual control is accomplished through the use of 4 pushbuttons for "clear," "readout," "enter," and "hold," respectively; in addition, 10 pushbuttons for the digits 0 to 9 and 2 pushbuttons for arithmetic signs are available.

The readout consists of an EL nine-window display. Three digits are used to display, in octal form, the address of the memory location into which information is to be inserted or from which information is to be extracted. Six digits, the first being the arithmetic sign, are used to display numeric information. Information transfer from the DEDA to the AEA is accomplished by means of a 36-bit serial digital word. Display parameters from the AEA are updated twice per second. The DEDA weighs 3.4 kilograms (7.5 pounds); the dimensions are 14.0 by 15.2 by 13.18 centimeters (5.5 by 6.0 by 5.19 inches). The operating power is 10 watts supplied by the AEA. The DEDA is mounted without cold rails in the LM cabin.

Abort sensor assembly. - The ASA is a strapped-down inertial-sensor unit mounted to the LM structure and oriented with the coordinate reference axes along the vehicle axes. The ASA senses and measures accelerations along and angular rotations about the LM axes, converts these motions to discrete increments, and transmits these increments in the form of pulses to the AEA for processing. The ASA consists of three floated, pulse-rebalanced, single-degree-of-freedom, rate-integrating gyros; three pendulous, fluid-damped accelerometers and associated pulse torquing electronics; a frequency countdown subassembly; coarse and fine temperature controller units; a power supply; and interface electronics.

The ASA uses current pulse torquing to rebalance the output from the sensors. Vehicle motions detected by the sensors are converted to alternating-current voltages having a magnitude and a phase proportional to the sensed motion. The output of each gyro is applied to a pulse torquing servoamplifier (PTSA) that quantizes the signals and provides output pulses to the AEA at 64 000 pulses/sec and to the sensor for torque rebalancing at 1 kilohertz.

The gyros used in the ASA were specifically developed for the strapped-down use. The accelerometers used are 2401 accelerometers that replaced the Bell VII units because of contamination experienced with those units. The sensors and their associated electronics are mounted orthogonally on a beryllium block for temperature control. Operating temperature is maintained by single-point control and is provided by two devices: a fast warmup control to provide minimum timelag to full operational capability and a fine temperature control to maintain the critical operating temperature of 322 K (120° F). Two sensors, placed mechanically in diagonal legs of a bridge, are used to detect temperature variations.

Both gyros and accelerometers operate on a torque-balance principle and use common pulse torque servoamplifiers. Time-modulated current is used to offset input angular rates and accelerations by a forced limit-cycle pulse torquing system. Binary torquing using alternate positive- and negative-current periods rather than discrete pulses provides a high angular information rate and a low system switching rate. Pulses from the pulse torque servoamplifiers to the AEA are quantized at 2^{-16} rad/pulse for the gyros and at 0.000952 m/sec/pulse (0.003125 ft/sec/pulse) for the accelerometers and are supplied at a maximum rate of 64 000 pulses/sec.

The necessary mounting accuracy of the ASA is obtained mechanically within 2 arc-minutes through four machined feet mounted to the LM navigation base outside and above the LM cabin. A side-mounted coldplate is used in the ASA for heat removal. The ASA weighs 9.4 kilograms (20.7 pounds) and has dimensions of 12.9 by 22.8 by 29.2 centimeters (5.1 by 9.0 by 11.5 inches). The ASA power dissipation is 74 watts.

The ASA specification values for inertial performance used in the development of the ASA are given in table I. (See fig. 2 also.) The ASA specification criteria are augmented by parameter stability criteria that are exclusively for bench-test maintenance-equipment calibrations at one facility. The test limits are given in table II. A repeatability limit on the three readings used to determine a mean representing the parameter value for any one calibration run is also required for a bench calibration. These limits are given in table III.

TABLE I. - ABORT SENSOR ASSEMBLY SPECIFICATION VALUES

Parameter	Channel	Trim value	Trim stability	
			Limit	Days
Gyro scale-factor error	X, Y, Z	4500 pulses/min	±870 pulses/min	120
Gyro bias	X	2.4 deg/hr	±2.8 deg/hr	120
	Y	2.4 deg/hr	±.85 deg/hr	8
	Z	2.4 deg/hr	±.67 deg/hr	3
Gyro input axis (IA) mass unbalance	X, Y, Z	4 deg/hr/g	±2.3 deg/hr/g	120
Gyro spin axis (SA) mass unbalance	X, Y, Z	4 deg/hr/g	±2.3 deg/hr/g	120
Gyro Y-axis alinement	X	130 arc-sec	--	--
Accelerometer Y-axis alinement	X	250 arc-sec	--	--
Gyro Z-axis alinement	X	250 arc-sec	--	--
Accelerometer Z-axis alinement	X	250 arc-sec	--	--
Gyro X-axis alinement	Y	130 arc-sec	--	--
Accelerometer X-axis alinement	Y	130 arc-sec	--	--
Gyro Z-axis alinement	Y	250 arc-sec	--	--
Accelerometer Z-axis alinement	Y	250 arc-sec	--	--
Gyro X-axis alinement	Z	130 arc-sec	--	--
Accelerometer X-axis alinement	Z	130 arc-sec	--	--
Gyro Y-axis alinement	Z	130 arc-sec	--	--
Accelerometer Y-axis alinement	Z	250 arc-sec	--	--
Accelerometer scale-factor error	X, Y, Z	4500 pulses/min	±940 pulses/min	120
Accelerometer bias discrepancy	X, Y	600μg	585μg	120
	Z	--	113μg	3
Accelerometer bias discrepancy	X, Y, Z	100μg	--	--
Gyro bias discrepancy				
Input vertical minus output vertical	--	.2 deg/hr	--	--
Spin vertical minus output vertical	--	.2 deg/hr	--	--
Output up minus output down	--	.33 deg/hr	--	--
Gyro scale-factor nonlinearity	X	0 to 10 deg/sec	180 pulses/min	--
	Y	10 to 22 deg/sec	200 pulses/min	--
	Z	22 to 25 deg/sec	580 pulses/min	--
Accelerometer scale-factor nonlinearity	X, Y, Z	100μg	--	--
Gyro scale-factor asymmetry	X, Y, Z	(a)	--	--
Accelerometer scale-factor asymmetry	X, Y, Z	200μg	--	--

[a]See figure 2.

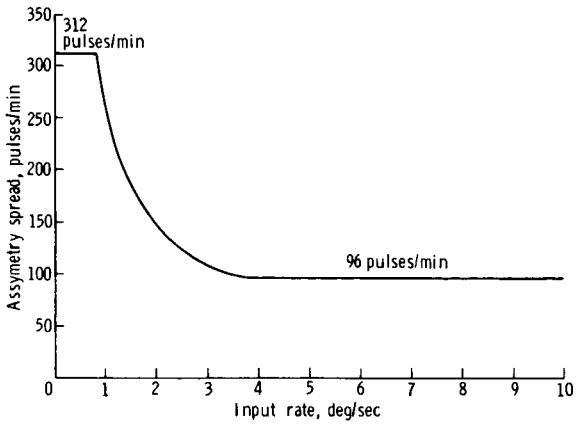

Figure 2. - Abort sensor assembly asymmetry requirements.

Because of the fixed nature of a strapped-down guidance system, complete calibrations requiring rotation cannot be performed in a vehicle. However, an Earth prelaunch calibration (EPC) program used in the AEA provides a determination of gyro drift when vehicle azimuth and latitude are known. In addition to the specification requirement, the time-stability values of table IV were generated on the basis of the AGS estimated capability in flagging non-characteristic EPC results.

TABLE II. - ABORT SENSOR ASSEMBLY TIME-STABILITY LIMITS

Parameter	Channel	Symbol	Unit	Limit on delta-mean for time interval, days								Shipment delta	
				0 to 2	2 to 6	6 to 10	10 to 20	20 to 40	40 to 60	60 to 90	90 to 120	From HSSC[a] to KSC	From BPA[b] to KSC
Gyro bias	X, Y, Z	B^G_{XI}, B_{YO}, B^G_{ZO}	deg/hr	0.35	0.48	0.54	0.60	0.64	0.66	0.69	0.73	--	--
Gyro scale factor (2.62 deg/sec)	X, Y, Z	S^G_i	pulses/min	160	195	240	300	300	300	300	300	--	--
Gyro spin mass unbalance	X, Y, Z	U^S_i	deg/hr/g	.36	.44	.53	.66	.88	1.03	1.19	1.30	--	--
Gyro input mass unbalance													
X gyro[c]	X	U^I_X	deg/hr/g	.30	.35	.45	.64	.90	1.10	1.35	1.56	--	--
				-.30	-.48	-.57	-.86	-1.28	-1.63	-2.01	-2.39	--	--
Y, Z gyro	Y, Z	U^I_i		.25	.35	.45	.64	.90	1.10	1.35	1.56	--	--
Gyro misalinement[d]	XY, XZ YZ, YX ZX, ZY	γ_{ij}	arc-sec	46	46	46	46	46	46	46	46	80	60
Accelerometer bias, IA	X, Y, Z	B^A_{iI}	ug	e_{90}	e_{140}	e_{155}	e_{170}	195	215	240	264	--	--
Accelerometer scale factor[c]	X, Y, Z	S^A_i	pulses/min	e_{80}	e_{80}	e_{80}	e_{80}	80	80	80	80	--	--
				e_{-90}	e_{-110}	e_{-137}	e_{-192}	-280	352	-445	-506	--	--
Accelerometer misalinement	XY, XZ YZ, YX ZX, ZY	α_{ij}	arc-sec	46	46	46	46	46	46	46	46	80	60

[a] HSSC = Hamilton Standard System Center.

[b] BPA = Bethpage, New York (location of Grumman Aerospace Corporation).

[c] Applies only after 60 days from sensor acceptance.

[d] The limit of 46 can be increased to 180 if an output-axis (OA) apparent misalinement problem has been demonstrated to exist.

[e] Smaller than acceptance test limits.

TABLE III. - ABORT SENSOR ASSEMBLY REPEATABILITY LIMITS

ASA parameter	Symbol	Unit	Limit on delta-measurements within a set of 3 calibrations	Limit on standard deviation σ from a set of 3 calibrations
Gyro bias	B^G_{iI}, B^G_{iO}, B^G_{iS}	deg/hr	0.29	0.17
Gyro scale factor (2.62 deg/sec)	S^G	pulses/min	112	66
Gyro IA mass unbalance	U^I_i	deg/hr/g	.22	.13
Gyro SA mass unbalance	U^S_i	deg/hr/g	.30	.18
Gyro IA misalinement	γ_{ij}	arc-sec	[a]25	[a]15
Accelerometer bias	B^A_{iI}	μg	42	25
	B^A_{iO}	μg	76	45
	B^A_{iP}	μg	76	45
Accelerometer scale factor	S^A	pulses/min	22	13
Accelerometer IA misalinement	α_{ij}	arc-sec	20	12

[a]The limit on σ for gyro misalinements γ_{XZ}, γ_{YX}, and γ_{ZX} can be increased to 106 arc-sec and the limit on delta-measurements to 180 arc-sec for a demonstrated OA apparent misalinement problem.

TABLE IV. - EARTH PRELAUNCH CALIBRATION TIME-STABILITY LIMITS

Parameter	Channel	Symbol	Unit	Limits on delta-measurements (or PIC[a] means) for time interval, days						
				0 to 2	2 to 6	6 to 10	10 to 20	20 to 40	40 to 60	60 to 90
Zero sway (MSOB[b]) EPC-PIC	X	B_X^G	deg/hr	0.54	0.68	0.78	0.91	1.10	1.24	1.39
	Y, Z	B_Y^G, B_Z^G	deg/hr	.40	.52	.58	.63	.67	.69	.72
EPC-EPC	X	B_X^G	deg/hr	.56	.70	.80	.93	1.12	1.25	1.40
	Y, Z	B_Y^G, B_Z^G	deg/hr	.44	.54	.60	.65	.69	.71	.74
Maximum sway (pad) EPC-PIC	X	B_X^G	deg/hr	.54	.68	.78	.92	1.11	1.24	1.39
	Y, Z	B_Y^G, B_Z^G	deg/hr	.46	.57	.62	.67	.71	.72	.75
EPC-EPC	X	B_X^G	deg/hr	.58	.71	.81	.94	1.13	1.26	1.41
	Y, Z	B_Y^G, B_Z^G	deg/hr	.55	.64	.68	.73	.76	.78	.81

[a]PIC = Preinstallation calibration.

[b]MSOB = Manned Spacecraft Operations Building.

Test Program

The test program for the AGS consisted of design feasibility and verification testing, qualification testing, spacecraft testing, full mission engineering simulation (FMES), certification test requirements, and acceptance testing.

Design feasibility and verification tests. - Design feasibility tests were incorporated into the AGS program for component and part selection; for investigation of the performance of breadboard models, components, and subassemblies under various environmental conditions; for selection of materials; and for substantiation of safety margins and other analytical assumptions. The feasibility tests were conducted exclusively by the assembly vendor in support of design. Design verification tests were included in the program to substantiate the correctness of the assembly design for the intended mission under simulated ground and flight environments and off-design conditions.

Four assemblies were initially designated as reliability test models and assigned to design verification testing. Because the program schedule and cost considerations necessitated a reduction in hardware, only two assemblies were assigned to design verification testing. The first unit was assigned to critical environments, electromagnetic interference (EMI), and overstress testing. Critical environments were to be selected by the vendor to ensure that the assembly would pass the design-limit qualification test. During this test, the environments were to be increased from mission levels to twice mission levels. The overstress test was to be performed until failure and was to use launch or mission environments exclusively. Failure-mode prediction analysis was to be used in selecting the overstress environments. The second design verification test (DVT) unit was assigned exclusively to mission simulation in the order in which the environments were to be experienced.

Program constraints, primarily schedule problems, resulted in cutting the DVT program to one assembly and restricting the tests to design-limit environmental levels. Preproduction units were used for design verification testing, although the program goal was to use production hardware. The DVT environments for the AGS are given in table V.

In addition to design verification testing, a series of design-proof tests was performed on the AGS to evaluate interfaces, angular vibration, gyro scale-factor asymmetry, EPC (with and without sway), navigation in static and dynamic environments, in-flight calibration (IFC), resonance (3 hertz), coning, constants polarity, and flight-configuration compatibility (test set compared to flight-configuration performance).

TABLE V.- DESIGN VERIFICATION TESTING ENVIRONMENTS FOR THE AGS

Environment	Abort electronics assembly	Data entry and display assembly	Abort sensor assembly
Thermal vacuum	X	X	X
Resonance search	X	X	
Temperature vibration	X	X	
Shock	X	X	
Temperature/humidity	X	X	
Acceleration	X	X	
Leak		X	
Corrosive contaminants		X	
Oxygen		X	
Vibration			X
Gyro and accelerometer scale-factor linearity			X
Gyro and accelerometer mechanical frequency response			X
Angular vibration			X
Frequency response			X
Saturation and bottoming			X
Calibration transients			X
Magnetic field susceptibility			X

Qualification. - Two production AGS units were assigned to qualification testing. The qualification program was originally divided into two phases, qualification and postqualification, with a teardown and inspection between the tests.

The first qualification unit was assigned to simulate the mission environment. Ground environment tests were to be performed first, followed by two flight environment simulations. The postqualification testing was to consist of two additional flight simulations. The second unit was assigned to design-limit testing and unique environments, such as salt spray. The postqualification test for this unit was to be two overstress tests.

A ground rule of the test program was that the entire DVT program be completed before the beginning of qualification testing. Because of schedule considerations, design verification testing and qualification testing overlapped; this rule was modified for the AGS so that an environment was tested in design verification testing before the same environment was demonstrated in qualification testing.

Program cost and schedule considerations resulted in the elimination of postqualification testing. The number of flight simulations was also reduced, and the exposures were lengthened accordingly because of the time for setup and teardown of a test and the potential damage resulting from the activity.

In the endurance qualification, a 1000-hour burn-in before starting the environment tests was established to simulate the assembly test and checkout period. Because of schedule constraints, this period was reduced to 250 hours, and EMI testing was performed during the period.

The AGS qualification history consisted of the following separate tests.

1. ASA original qualification
2. ASA accelerometer change qualification
3. DEDA original qualification
4. DEDA modified EL display mounting qualification
5. AEA original qualification
6. AEA modified internal clock qualification
7. AEA increased vibration levels qualification
8. AEA modified memory read/write clock qualification

The multiple qualification tests were performed because of design changes as noted. Qualification testing was monitored by periodic test reviews at the vendor facility during the testing.

Spacecraft testing. - The subsystem checkout at the prime contractor and at the NASA John F. Kennedy Space Center (KSC) was controlled through a test and checkout requirements document for each spacecraft. The test criteria for each vehicle were supplied to KSC by means of a test and checkout specification and criteria document. The KSC response to the MSC test requirements document, outlining the details of the tests to be performed, was stated in the test and checkout plan. Operational checkout procedures controlled the detailed procedures for each test.

Full mission engineering simulation. - The prime contractor's FMES was used to integrate AGS hardware and software into a closed-loop, six-degree-of-freedom simulation with other flight control hardware and software. The ASA was mounted on a flight-attitude table, and all hardware functions were used except the accelerometer outputs, which were necessarily simulated for input to the AEA. An extensive test program was performed on the AGS software baseline, the design mission computer program (DMCP), followed by tests of each flight program with hardware. Gyro mass unbalance proved to be a significant error source that could not be eliminated in the dynamic tests without complex compensations that were not readily available. Before activation of the FMES facility, a three-degree-of-freedom test was performed on a preproduction unit to verify the stability of the attitude-control loop.

Certification test requirements. - A series of performance demonstrations was set up in the program as constraints on flight. These tests required formal approval of the test plans, or certification test requirements, and formal approval of the documented test results, or certification test endorsements. The AGS certification requirements included qualification testing of the ASA, the AEA, and the DEDA, and demonstration of the AGS EPC, in-flight gyro calibration, mission performance for the LM-3 Earth-orbit mission, mission performance for the DMCP software program, lunar mission performance, and in-flight accelerometer calibration. To avoid redundant testing, functions normally evaluated as part of vehicle checkout were not performed as certification test requirements.

Acceptance tests. - One major change in acceptance testing was made when the vibration levels for each operating assembly were changed from 3g root-mean-square random vibration to 6.6g root mean square. The change was made to ensure adequate workmanship rather than to reflect the worst mission environment (approximately 3g root mean square). The acceptance tests performed on the assemblies are given in table VI. Additionally, as a part of acceptance for initial deliveries that were accepted as a system, a compatibility test was performed using the three assemblies that comprise the AGS. The tests performed on the AGS consisted of three sets of calibrations: a lunar aline, an attitude reference exercise, and a connector waveform test.

TABLE VI. - ACCEPTANCE TESTS PERFORMED ON THE AGS

Test	Abort electronics assembly	Data entry and display assembly	Abort sensor assembly
Vibration	X	X	
Thermal vacuum	X		X
Detailed operational	X		
Hardwired memory	X		
Waveform and power supply regulation	X		
Operational		X	
Six-position pushbutton activation		X	
Low-level vibration and pushbutton activation		X	
Temperature		X	
Leak[a]		X	
Luminescence and pushbutton force		X	
Warmup			X
Test connector on/off and calibration			X
Gyro scale-factor linearity and asymmetry			X
Vibration (launch and boost) and calibration			X
Servomotor frequency response			X
Gyro runup and calibration			X
Vibration (ascent/descent) and calibration			X
Pulse moding			X
Gyro and accelerometer scale-factor linearity and asymmetry and calibration			X
Angular vibration			X
Accelerometer pendulum static friction test and calibration			X
Gyro scale-factor linearity and asymmetry			X
Calibration			X

[a]To detect leaking pushbuttons, this test was performed in a vacuum and expanded from 1 to 5 hours.

Software Development

Software development included the formulation of basic requirements and development procedures, verification methods, and use of the software.

Software functional description. - The following basic mission requirements governed software development.

1. Orbital insertion shall be achieved within a pericynthion greater than 9144 meters (30 000 feet).

2. Abort to rendezvous from any point in the LM mission shall be accomplished within the LM fuel budget. The total ascent differential velocity (delta-V) is 1946 m/sec (6386 ft/sec), subtracting 7.6 m/sec (25 ft/sec) for docking.

3. The maximum navigation error incurred during powered descent, hover, and powered ascent shall not exceed 762 meters (2500 feet) and 1.2 m/sec (4 ft/sec).

4. The AGS must bring the LM within a 9.3-kilometer (5 nautical mile) sphere of the CSM with a navigation velocity error of less than 9 m/sec (30 ft/sec).

The fuel constraint proved to be variable because as vehicle weight increased in the course of the program, the available delta-V decreased. The delta-V available for rendezvous after insertion, the prime consideration, decreased from 155 m/sec (509 ft/sec) to 106 m/sec (349 ft/sec) during the program. To satisfy the software requirements, the following capabilities were necessary.

1. Navigation of the LM and CSM vehicles

2. Initialization of the LM and CSM state vectors

3. Alinement of the inertial reference to a selected coordinate system

4. Maintenance of vehicle attitude information with respect to inertial space

5. Steering of the vehicle

6. Calibration and compensation of gyro and accelerometer parameters

7. Solution of the guidance equation

8. Generation of monitoring data for displays and telemetry

9. Automatic in-flight check of computer memory and logic

To satisfy these requirements, the functions of navigation, alinement, calibration, radar data processing, guidance routines, and attitude and engine control were implemented.

Navigation is performed in the AGS inertial reference frame with the origin at the center of the attracting body. Sensed velocity increments from the ASA are transformed from body to inertial coordinates and used in the navigation computations when a threshold is exceeded. The threshold prevents the integration of accelerometer bias during coasting flight. The velocity changes caused by gravity are computed, assuming a spherical gravity model for the attracting body. State vector initialization information on the LM and the CSM is obtained from a hardwire interface with the PGS telemetry downlink. If the PGNCS is not operational, the data are inputted through the DEDA. The absolute time of the AGS is initialized through the DEDA. A time bias exists between the AGS and the mission time because of AGS time-register limitations. Initially, LM time was to be based on manning in lunar orbit; a change to mission time initialized at Earth lift-off required a fixed AGS time bias. The time bias is kept in the PGS, and epoch time for AGS initialization has this bias subtracted before being placed on the primary guidance downlink.

Alinement consists of updating the AEA direction cosine matrix by one of three methods provided. The normal alinement frame is the landing site local vertical. The X-axis passes through the landing site to the center of the Moon, the Z-axis is defined by the vector product of the X-axis and the CSM angular momentum vector, and the Y-axis completes the orthogonal triad. The PGNCS provides continuous attitude information to integrator registers in the AEA by means of hardwired connections from coupling data units for the three primary system gimbal angles. Although the AGS maintains continuous knowledge of the primary guidance alinement, the AEA direction cosine matrix is updated with the information only on DEDA command. A second alinement capability is that of lunar aline, in which ASA accelerometers are used to determine local vertical with respect to vehicle coordinates on the lunar surface. Azimuth information is supplied from a quantity stored at touchdown or from a DEDA input. An azimuth correction factor can be inputted to correct for lunar rotation during the stay time or to correct for a CSM plane change. The third alinement mode is body-axis aline in which the direction cosine matrix is set to the body reference frame.

Three calibration options are available in the AGS software. The gyro and accelerometer calibration option is designed for orbital operations. The gyros are calibrated to the PGS over a 5-minute period, and the accelerometer readings in free fall are compensated during a 30-second period. During in-flight calibration, jet firings are inhibited for accelerometer calibration, and vehicle rates are held below 0.075 deg/sec for gyro calibration. The second calibration option is lunar surface gyro calibration, which requires 5 minutes. The program initially stores the existing direction cosine matrix as a reference for computing drift compensation. The input angular increment is corrected for lunar rotation rate. In the third option, the accelerometers are calibrated only in free fall during a 30-second period.

Radar data are inputted through the DEDA to reduce the error in the LM state with respect to the CSM. The radar data inputted through the DEDA are range and range rate after nulling the radar pointing error with respect to the Z-axis and storing the direction cosine. A minimum of six range/range-rate updates at intervals of 4 minutes is required for an accurate update. For ranges as long as 741 kilometers (400 nautical miles), nine updates are required.

The five guidance options available are as follows.

1. The orbital insertion option provides steering and engine cutoff for inserting the LM into a desired lunar orbit.

2. The concentric sequence initiate option computes the horizontal burn required to satisfy targeting conditions, the desired terminal phase initiate (TPI) time, and the TPI line of sight to the CSM for a final orbit transfer to the CSM.

3. The constant differential height (CDH) routine computes the burn direction and magnitude required to make the LM and CSM orbits coelliptical at a predicted CDH time.

4. The TPI routine calculates the transfer burn for placing the LM on a direct intercept trajectory with the CSM based on a fixed transfer time.

5. The external delta-V routine accepts components of a velocity-to-be-gained V_G vector input through the DEDA. The vehicle is pointed along the vector and maintained in a local-horizontal system in real time.

Attitude errors are generated by the AEA in accordance with selected control modes. During attitude reference alinement and calibration, the errors are set to zero. In the attitude-hold mode, the attitude errors cause the vehicle to remain at the attitude existing when the mode was entered. In the guidance mode, the attitude errors cause the vehicle to steer in accordance with the guidance equations. In the acquisition mode, the attitude errors cause the vehicle Z-axis to point toward the CSM to facilitate radar acquisition.

An engine-on command from the AGS is issued only after a set of constraints has been satisfied; abort or abort stage is commanded, a preset duration of ullage is sensed, the automatic discrete is present, guidance control is set to AGS, and guidance steering is selected through the DEDA. During powered descent, the ullage constraint is removed by DEDA command so that, near the lunar surface, ignition of an engine may be instantaneous in the event of a flameout.

Displays of total attitude, attitude errors, altitude, altitude rate, and lateral velocity are computed and outputted from the AEA for crew monitoring. The AGS outputs a digital telemetry list of 50 words each second for the monitoring of AGS status and performance.

A ground-support-equipment (GSE) service routine for loading the AEA memory, a DEDA processing routine for AEA/DEDA communications, and an in-flight self-test routine for checking the AEA memory and logic comprise the major software functions.

Software development, verification, and use.- The software developed for the AGS was obtained by MSC through a direct contract with the subcontractor. Integration with the hardware program was obtained by using an AGS performance and interface specification for software development maintained by the prime contractor and by requesting that the subcontractor hardware program manager be appointed task manager for AGS software development.

A deliverable program, including mission constants and ASA hardware compensation constants, was established for each flight for the softwired 2048 words of the AGS memory. The individual flight programs were amended versions of a DMCP delivered in March 1967. This program, although nonflight, was used in the contractor's six-degree-of-freedom simulation facility to verify AGS performance of the reference mission and to satisfy the AGS system responsibility of the contractor.

The planned software development at program initiation was based on a series of five design reports spaced over 11 months from the software vendor in response to and interleaved with three data packages from MSC to the vendor. The five design reports consisted of the following documents: Design Report (DR) 1 - Preliminary Analysis Report; DR 2 - Program Specification and Equation Test Plan; DR 3 - Equation Simulation Results Summary, Equations Document, Operating Procedures, Program Checkout Plan, and Performance Analysis Report; DR 4 - Program Checkout Results Summary and Program Verification Test Plan; and DR 5 - Program Verification Test Results Summary, Programed Equations Document, Performance Analysis Review Report, Program Listing, Binary and Symbolic Card Decks, and Program Tape.

The three MSC data packages contained special mission requirements and the refined mission trajectory consisting of the mission preliminary reference trajectory, the reference trajectory, and the operational trajectory. The AGS software performance and interface specification contained all other information required for software development.

Because the number of design reports proved unwieldy and excessively time consuming, five reports were combined into three. The development schedule was then revised, as follows, in terms of time before launch.

1. At 12.5 months before launch, MSC data package 1, containing the preliminary reference trajectory and the mission requirements, is delivered to the subcontractor.

2. At 11 months before launch, subcontractor DR 1, containing the program specification and the preliminary AGS mission performance analysis, is delivered to MSC.

3. At 10.5 months before launch, MSC performs a critical design review of DR 1.

4. At 8 months before launch, MSC data package 3, containing the mission reference trajectory, is delivered to the subcontractor.

5. At 7 months before launch, subcontractor DR 2, including the equation test results, a verification test plan, and a preliminary program, is delivered to MSC.

6. At 6.5 months before launch, MSC performs the first article configuration inspection (FACI) of DR 2.

7. At 5 months before launch, subcontractor DR 3, consisting of a verified flight program and related documentation, is delivered to MSC.

8. At 4.5 months before launch, MSC performs a customer acceptance readiness review (CARR) of DR 3.

9. At 3 months before launch, MSC data package 3, containing the operational flight trajectory, is delivered to the subcontractor.

10. At 2 months before launch, the subcontractor performs the final performance analysis based on data package 3, and MSC performs the flight readiness review (FRR).

11. At 1.5 months before launch, the subcontractor delivers the final program constants tape for computer loading.

After delivery of the baseline program, the development procedure for the balance of the flight programs was shortened to begin at 9 months before launch and simplified as follows.

1. At 9 months before launch, the MSC data package, containing mission requirements and the reference trajectory, is delivered to the subcontractor.

2. At 8 months before launch, the subcontractor interim design report, containing the program status, the verification test plan, and the performance analysis test plan, is delivered to MSC.

3. At 7.5 months before launch, MSC performs the FACI review of the interim design report.

4. At 6 months before launch, the subcontractor delivers preliminary flowchart changes, operating procedures changes, and a final computer program specification. The unverified program is deliverable at this time for incorporation in the prime contractor FMES and the MSC hybrid simulation.

5. At 5 months before launch, the subcontractor delivers the program, including verification test results, performance analysis results, the programed equations document, the operating manual, and a design report. The program is delivered in the form of a binary deck and listing, a bench-test equipment loading tape, and an acceptance checkout equipment (ACE) tape for vehicle use.

6. At 4.5 months before launch, MSC performs a CARR of the program delivery package.

7. At 8 weeks before launch, the MSC operational trajectory, mission data, and constants are supplied to the subcontractor.

8. At 5 weeks before launch, the subcontractor delivers the final flight program with updated constants in ACE format and the final performance analysis. An FRR is performed at MSC. Before subcontractor submittal of documentation, an internal subcontractor software review board approves the release.

The performance analysis performed for program delivery 5 months before launch consisted of Monte Carlo runs using the ASA specification error model and the ASA capability estimate error model in mission simulations. The mission simulation cases selected were the most stringent and always included abort from hover. The performance analysis performed 5 weeks before launch used an error model generated from data taken on the flight model ASA.

Verification of proper computer loading was accomplished in the following manner. The flight program card deck delivered at the CARR was transposed by the prime contractor to an ACE tape or the format used to load the AEA by the ACE computer at KSC. The prime contractor ACE tape was transmitted to the subcontractor for independent verification and then sent to KSC. The final AEA dump, after loading with the constants-updated program in ACE format (supplied by the subcontractor 5 weeks before launch), was compared with the prime-contractor-generated ACE tape, and the noncomparing memory locations (noncompares) were printed out. The noncompares, which represent the updated mission constants, were compared with a list of expected noncomparing locations supplied by the subcontractor at the time of the FRR. An additional verification procedure for comparing the original subcontractor binary card deck with the final memory dump was also followed for the first flight but was discarded for later flights because of redundancy.

The verification procedures used in the course of program development by the subcontractor consisted of equation testing, program checkout, verification testing, and performance analysis. Scientific or engineering simulations of the equations in a closed-loop configuration were designed to demonstrate equation performance under both nominal conditions and vehicle, sensor, or trajectory dispersions of 3 standard deviations (3σ). Testing of the coded program was performed by using a bit-by-bit interpretive computer simulation (ICS). This check verified that the program was implemented in accordance with the equations.

A closed-loop interpretive simulation of the AEA program and the vehicle flight characteristics (ICS flight simulator (FS)) was used in verification testing. Verification that the program was capable of guiding and controlling the vehicle in all operating modes was accomplished. Special ICS driver routines also were formulated to augment this test. A Monte Carlo analysis program using 600 cycles was performed to determine detailed AGS performance compared to mission requirements.

Verification also was performed at MSC by using a hybrid computer facility with actual ASA and DEDA hardware for independent test cases and by using special test cases in the subcontractor ICS/FS program. Additional testing for each mission was performed by the prime contractor with a six-degree-of-freedom computer simulation incorporating the AGS as well as other hardware components in the LM flight control system.

The selection of hardware compensation constants for the final program tape was made after examination of the data history of the actual flight ASA. In all cases, the examination resulted in the selection of the final bench calibration values with the exception of the accelerometer scale factor, which was extrapolated to the time of the mission. The predictable effects of magnet aging on the accelerometer scale factor

enabled this extrapolation. The gyro values were checked by Earth prelaunch calibrations performed after final ASA installation in the vehicle. The EPC uncertainty of 0.37 deg/hr and the stability exhibited by the ASA led to maintaining the compensation values at those obtained by the more accurate bench calibration. In-flight calibration of gyro and accelerometer biases before undocking in lunar orbit allowed final compensations for the mission.

Other software deliverables supplied to MSC were EPC tapes and simulated flight procedures. Earth prelaunch calibration was a 20-minute special program for determination of gyro drift in the vehicle sway environment. The other ASA parameters used in the EPC tape for compensation were derived from data taken during the first ASA bench calibration at KSC.

The simulated flight program consisted of a set of procedures used with a specified flight program to simulate various mission phases. The purpose of the simulated flight was to gain confidence in AGS operation with interfacing LM subsystems. Simulated flight procedures of the AGS were designed to test AGS simulated flight initialization; CSM acquisition; radar filter; abort from powered descent; abort from the lunar surface; and coelliptic sequence initiate (CSI), CDH, TPI, and external delta-V guidance solutions. The criteria for the tests were obtained from interpretive computer simulations and resulted in value bounds or bounded curves for various AEA and display parameters. Simulated flights were performed throughout AGS testing as an integral part of operational checkout.

Software changes were accomplished through the submittal of software change proposals generated independently or on request by the software vendor. A formal MSC board, controlling both AGS and PGNCS software, reviewed the software change proposals.

Abort Guidance System Mission Revisions

Revisions to the AGS mission are discussed in the following paragraphs. The major change consisted of replacement of the direct-ascent trajectory for rendezvous with the coelliptic flight plan.

Direct ascent. - The first AGS rendezvous concept was a minimum-time, direct-ascent trajectory to the CSM following abort. The CSM orbital altitude for this mission was 148 kilometers (80 nautical miles). For CSM phase angles that precluded direct ascent, the AGS was placed in a parking orbit at the insertion altitude and then at 15 240 meters (50 000 feet) to obtain the maximum catchup rate to the CSM. Data for orbital transfer to the CSM were obtained from external sources.

Coelliptic flight plan. - In January 1966, the direct-ascent concept was discarded and replaced by the coelliptic flight plan, which essentially provided for an LM parking orbit for all ascent cases. The CSM orbital altitude was changed to 111 kilometers (60 nautical miles) for this procedure. A diagram of the coelliptic sequence is given in figure 3.

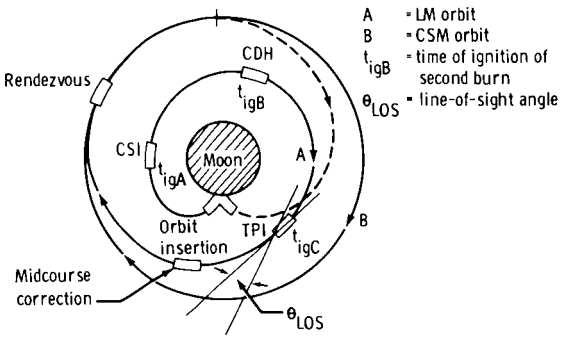

Figure 3.- Coelliptic rendezvous flight profile.

The AGS, following abort or ascent from the lunar surface, inserts the LM into a lunar orbit based on insertion altitude, insertion altitude rate, and desired lunar orbit, usually 17 by 56 kilometers (9 by 30 nautical miles), under automatic control. The LM coasts until the time of ignition of the first burn t_{igA}, which places the LM approximately 90° from the insertion point. At that time, the rendezvous profile is initiated with the CSI maneuver. The burn is normally done in the external delta-V mode using the reaction control system (RCS), as are all burns of the rendezvous sequence. The CSI burn magnitude is determined by an iterative technique such that a desired relationship between the CSM and the LM exists at a specified time (time of ignition of the third burn t_{igC}) following a maneuver to produce a CDH between the CSM and the LM. The CDH burn following CSI is performed at the predicted time of LM orbit apofocus (or perifocus). Because of this burn, the LM orbit becomes coelliptic with that of the CSM, the line of apsides of the two orbits is alined, and a constant differential altitude between the two vehicles exists. The final planned burn of the sequence, TPI, is performed at the point at which a desired line-of-sight angle (usually 26.6°) between the LM and the CSM is reached. The magnitude is based on a fixed transfer time to rendezvous, usually equivalent to a 130° central angle transfer. The parameters of the transfer trajectory are determined by iteration to bring the LM to the predicted position of the CSM at the specified time. Two midcourse maneuvers are performed, as required, after TPI, and the burns are computed by the same technique used for the TPI maneuver. The braking maneuver for docking is originated at a range of 9.3 kilometers (5 nautical miles). A range and range-rate chart profile is followed, interleaved with nulling of the line-of-sight rate.

The sequence of events following an abort depends extensively on the time of abort. The nominal sequence outlined is used for aborts near the lunar surface. For aborts before powered descent, the TPI maneuver may be performed initially. The nominal sequence is also subject to extensive changes in the course of mission planning. A fixed or canned external delta-V maneuver can be performed before CSI; a dual CSI burn may be performed before CDH; and phasing maneuvers may be incorporated as requirements for landing site selection, rendezvous lighting, and rendezvous location dictate.

Mission Operation

The AGS is maintained operational in a ready state throughout the lunar mission as a backup to the PGS. A nominal operational profile is described in this section.

Lunar orbit. - The AGS is inoperative during the translunar-coast phase, and the ASA heaters maintain the ASA at a temperature of 322 K (120° F). Coolant is not supplied to the ASA coldplate. After the crewmen enter the LM in lunar orbit, the system is activated and the gyros are tested for a minimum of 25 minutes. An AEA self-test consisting of an AEA memory sum check and logic test is performed by DEDA command. The DEDA operation and the EL segment operation are verified. The AEA time is initialized by a DEDA entry, and an LM and CSM state vector initialization from the PGS downlink is performed. The AGS is then alined to the PGS, and the results are checked by monitoring the total-attitude indicators and the system digital downlink. The initialization of the AGS is checked by calling up the range and the range rate to the CSM and the in-plane angle between the Z-body axis and the local horizontal on the DEDA and by comparing the PGS readings. In-flight calibration of the AGS gyros and accelerometers is then performed.

Powered descent. - The gyro drift and navigation errors of the AGS are mitigated for the descent phase by a state vector initialization from the primary system 10 minutes before powered descent and by an alinement to the primary system 5 minutes before powered descent. During powered descent, the AGS is in the followup attitude reference mode because the primary system is in the vehicle-control mode. The AGS independently maintains an attitude reference, navigates, and solves the abort problem. The attitude, altitude, and altitude rates of the AGS are compared with those of the primary system during descent. The LM inertial velocity is displayed on the DEDA.

At an altitude of 1829 meters (6000 feet), the AGS navigation errors are further reduced by a DEDA altitude update. An AGS abort may be accomplished at any time by switching guidance control to AGS and pressing the abort button.

Lunar surface. - After touchdown, the AGS lunar surface azimuth is stored. Following a decision to stay, the LM state vector is initialized using information stored in the AEA before descent that reflects the lunar surface state, and the AGS is placed in lunar aline. When all systems are verified as operational, the AGS is initialized and alined to the primary system, the lunar azimuth is again stored, and an AGS lunar surface gyro calibration is performed. The AGS is then placed in standby with only the ASA operational for the duration of the stay on the lunar surface.

Before ascent, AGS time, state vectors, and alinement are again initialized, and a lunar surface gyro calibration is performed. The AGS is placed in lunar aline approximately 30 minutes before lift-off and is changed to guidance steering 2 minutes before lift-off to reduce gyro drift effects on the attitude reference.

Powered ascent. - During ascent, the AGS is in followup and is independently navigating and solving the insertion problem. The thrust axis V_G is monitored on the DEDA during the latter half of ascent. Initially, AGS total velocity is monitored. After insertion cutoff, the AGS velocity residuals in each axis are compared with the PGS and trimmed.

Rendezvous sequence. - After insertion, the AGS is updated in relation to the CSM by the insertion of radar range and range-rate information through the DEDA. The AGS facilitates rendezvous radar acquisition of the CSM by a mode that points the

vehicle Z-axis at the CSM. Nine range and range-rate points are required before the first coelliptic sequence maneuver, CSI; six points are required before each subsequent powered maneuver. The AGS independently solves for each powered maneuver and operates without dependence on the PGS after insertion for rendezvous.

Abort Sensor Assembly Development Problems

The following significant problems were encountered during the development of the ASA.

Initial accelerometer selection. - The Bell IIIB accelerometer was originally proposed for the AGS and approved. At the time of program initiation, however, strong arguments were advanced by the contractor for switching to the Bell VII, a new, scaled-down version of the Bell IIIB. Although the Bell IIIB operational and test experience was extensive during the Ranger Program and at the NASA Jet Propulsion Laboratory, the arguments for savings of 1.1 kilograms (2.5 pounds) in weight, 0.0005 cubic meter (29 cubic inches) in volume, and 4 watts of steady-state power were attractive. The deciding argument, however, was that hermetic sealing of the Bell IIIB would be expensive in terms of scheduling, requiring 16 weeks for delivery of an unsealed unit and 8 months for delivery of a sealed unit compared to 4 weeks for initial sealed Bell VII delivery. A change was made to the Bell VII unit. Subsequent events, however, revealed that the hermetic sealing of the Bell VII had not been adequately proved, and a redesign of the case was required to prevent "oil canning." Subsequent bias stability and contamination problems with the Bell VII have indicated that the original selection of the Bell IIIB accelerometer was correct.

Spin motion rotation detectors. - The necessity for monitoring gyro wheelspeed became apparent in the early stages of the program. Platinum cobalt slugs were added to the gyro wheels with a pickoff coil to generate a pulse for each wheel revolution. The spin motion rotation detectors also served to check wheel runup and rundown times and, therefore, bearing integrity.

Noise. - A general electronic noise problem within the ASA became apparent with the integration of the first ASA. Inertial performance changed when the test-connector outputs were capped instead of being connected to the test set. No single design change eliminated noise problems. Corrective actions taken included eliminating ground loops with the test set connected, rerouting sensitive internal leads, twisting instrument torquer leads instead of using shielded cable, using shields between the pulse torque servoamplifiers and the power supply, and connecting secondary power ground internally to chassis ground.

Temperature maintenance. - The ASA instruments were heated through a beryllium block rather than through individual sensor heaters. The beryllium block represented an extensive design task, requiring complex shaping and drilling to achieve proper heat transfer and thermal gradients. Nine designs for the beryllium block were required to achieve the final design.

Internal cabling. - Flexible, multilayer printed circuit cable was used in the interconnecting internal harnessing of the first preproduction ASA primarily because of the weight and volume limitations of conventional wiring. This method required more volume than anticipated, had an unsatisfactory appearance because the cable would not stay molded around corners, and was impractical from the standpoint of accommodating design changes. Conventional point-to-point stranded wiring in bundles was used in the second preproduction ASA.

Thermal design. - The ASA power supply was located between the main housing and the heat sink. The preproduction power supply was potted in a thermal conducting compound that allowed heat to permeate through the compound from the main housing and the power supply to the heat sink surface. The thermal conductivity of the potting compound, however, was not as high as anticipated (0.5 W/m-K (0.3 Btu/hr/ft-°F) compared to 36.5 W/m-K (21 Btu/hr/ft-°F)), and a weight penalty was incurred because of the dense potting compound. The production power supply was designed such that all significant heat-producing components and modules were heat sunk directly to the coldplate side of the power supply housing. A less dense potting compound could then be used with considerable weight reduction. Heat from the main housing was routed by two studs through the power supply to the coldplate surface. These studs incorporated adjustable slugs by which the thermal path between the main housing and coldplate could be varied. The capability of trimming total power consumption after ASA assembly was gained.

Mounting feet. - Each pair of preproduction ASA mounting feet was an integral unit at each end of the housing. Each foot contained a Mycalex ring that served as a thermal barrier, but machining the Mycalex was difficult. Because of continued exposure to the specified vibration environment, fatigue failures occurred. An individual suspension system was incorporated for the production design. Each foot was attached to the block with a thermal path small enough to eliminate the need for Mycalex. The body of each titanium foot was hollowed, and an aluminum slug covered with an elastomer was inserted to provide damping and to prevent exceeding the specification resonance requirements.

A second change was necessary when high resonances occurred as a result of elastomer deterioration caused by extended periods of vibration. Several other materials were tested for damping efficiency when inserted in the foot in place of the aluminum slug and the elastomer. Although analysis indicated otherwise, a solid titanium foot did provide adequate damping and was less difficult to manufacture. Solid titanium was incorporated into the foot design.

Cover support. - The preproduction ASA cover that served as the support member for the three connectors was undesirable structurally and time consuming to remove. A separate structural member was designed to support the connectors, and the cover was redesigned.

Accelerometer scale-factor temperature sensitivity. - The Bell VII accelerometer scale-factor temperature sensitivity was higher than tolerable. Temperature compensation was incorporated into the accelerometer design, but the accelerometer was later discarded because of contamination problems.

Thermal runaway. - A potential thermal runaway existed in the ASA design if the sensing thermistor controlling the fast warmup opened or if the trim resistor short circuited. This condition could endanger other equipment on the LM adjacent to the ASA. A normally closed thermostat set to open at a temperature of 339 K (150° F) (322 K (120° F) normal operation) and set to close at 328 K (130° F) was incorporated in series with the +12-volt ASA power supply caution-and-warning (C&W) signal. The ASA is turned off manually if the display indicates a malfunction on this line.

Accelerometer warmup. - The Bell VII accelerometer bias had an excessively long warmup time. The requirement for ±30μg of steady state in 25 minutes was violated by several hundred milligals (μg's) for several hours. The long warmup was caused by an electrostatic charge buildup between the capacitor plates and the torquer coil on the pendulum when the torquer coil potential was 16 volts above ground and by a change in the resulting electrostatic forces on the pendulum as the charge leaked off gradually.

The accelerometer torquer is operated at a 16-volt, direct-current potential relative to ground because of the PTSA design. This potential causes buildup of an electrostatic charge between the pendulum and the capacitor plates that is inversely proportional to the relative distance between them. When the pendulum is not physically centered, one plate exerts a greater force on the pendulum than the other. Because of low leakage rates of the bridge circuit capacitors, much time is required to null the electrostatic forces. The long time constant causes the effective bias to change proportionately.

Initially, a capacitor adjustment was made to bring the electrical null around which the accelerometer operates into coincidence with the electrostatic null. Bleed resistors were later added to drain the electrostatic charge.

Cover design. - Problems developed in building the single-piece ASA cover. The initial procedure was to build the inner skin first, bond honeycomb core material to it, and then bond the outer skin to the honeycomb. To facilitate manufacturing, the honeycomb core material was changed to polyurethane foam. The foam, however, separated at the bond line during extended vibration, and the core material was changed back to honeycomb.

Additionally, during environmental testing, pins from the electronic subassemblies shorted, through tolerance buildup, to the inner aluminum skin of the cover through an insulating fiberglass board. The inner aluminum skin of the cover was replaced with fiberglass. The thermal and EMI effects of the change were acceptable.

Thermal-vacuum effects. - Because of thermal-vacuum exposure as high as 0.7 deg/hr, gyro bias shifts occurred during initial ASA testing. The problem was first thought to be thermal because the temperature difference between the gyros and the mounting block increased as much as 1.1 K (2° F) under vacuum conditions. The gyro mounting holes were enlarged to minimize changes in heat flow across the airgap from the gyro case to the mounting block between ambient and vacuum conditions. This action did not correct the problem. A thermally conductive compound was then applied to the gyro seats to prevent the thermal resistance across the interface from being affected by pressure variations. This addition reduced the thermal-vacuum shifts below the 0.3-deg/hr specification.

Gyro mass unbalance instability. - Both long- and short-term mass unbalance instabilities became evident in the RI-1139B gyro. The long-term shifts violated the initial specification requirement of 2 deg/hr/g; thus, the use of mass unbalance became an uncertain indicator of bearing wear. The shifts were orientation dependent and predictable with orientation change. The cause of the shifts was presumed to be settling of the two-cut gyro flotation fluid under gravity conditions. Gyro circle tests were instituted during acceptance to determine that the shift magnitude was bounded, and the specification was relaxed to a value of 4 deg/hr/g. Because of the fixed sensors, the ASA has the advantage that only X-gyro-spin-axis mass unbalance (due to thrusting) is a significant error source in the mission. Corrective action was taken to store both the ASA units and the gyros before installation in a fixed orientation to eliminate the mass unbalance shifts. The ASA shipping container was modified to mount the ASA X-axis vertical, as it is mounted in the vehicle, rather than the previous Z-axis vertical. The gyros were preassigned a specific ASA axis and stored in the position before mass unbalance trim. After acceptance, they were maintained in the chosen position until ASA installation.

The short-term instability was observed during processing by the gyro manufacturer and the ASA vendor. Because of the different torquing methods used at the two installations, the shift was found. Analog torquing used by the manufacturer dissipated 0.7 watt. Pulse torquing used by the vendor put 1.3 watts in the torquer. The manufacturer corrected this discrepancy by performing the final mass unbalance adjustment with 1.3 watts dissipated in the torquer.

Gyro fluid contamination. - Erratic gyro drift was evident in the first units produced by the manufacturer. Particle contamination was found in three units. Extensive changes were made in quality control procedures, and improvements were made in the manufacturer's cleanroom facility. Fluid control was tightened, wax seals were eliminated from the fill system, a molecular seine was added, and a back pressure fill system was used.

Accelerometer bias instability. - Accelerometer bias shifts of several hundred milligals (μg's) were observed at the inception of the Bell VII program. Investigation of these shifts revealed that they were asymptotic and storage and temperature dependent and that a maximum shift of 900μg was possible over a 5-day period when stored with the input-axis up and then down and with the temperature maintained at 339 K (150° F). Reducing the storage temperature to 322 K (120° F), the ASA operating temperature, reduced the shift to 300μg peak to peak. The fixed ASA storage, adopted because of gyro mass unbalance shifts, also mitigated the problem. The shift was traced to the creep rate of the epoxy joint between the aluminum structure and the pendulum copper beryllium spring. The ASA shipping containers were modified to reduce the storage temperature from 339 K (150° F) to 322 K (120° F). The IFC of accelerometer bias, previously incorporated in the AGS software, contributed to eliminating the effects of the instability during the mission.

Accelerometer contamination. - A significant ASA problem developed because of contamination within the Bell VII accelerometer. The failure mode was the adhering of the accelerometer pendulum to one of the capacitive pickoff plates while in the off mode such that the 3g restoring force of the loop would not free it upon activation. The failures occurred on units that had been in the field for approximately 1 year. The

pendulums on two field units were definitely captured, and a third exhibited a tendency to stick. During analysis of the contaminant, two primary substances were noticed on the brass capacitive pickoff plates. One substance was a viscous film composed of amines from a catalyst used in curing the encapsulant for a transformer within the accelerometer. The second was a whitish growth composed principally of zinc chloride. Tests indicated that the contaminant could be grown on brass in the presence of contaminant sources. Dezincification of the brass would occur in the presence of chlorine and moisture.

A pendulum freedom test, open loop, was performed to screen the accelerometer. The test criterion was that the pendulum fall free from a capacitive pickoff plate within 6° of vertical. Of the 26 units tested, 15 exhibited a degree of stickiness. An outgassing procedure was incorporated to eliminate the contaminant. All seven units committed exhibited stickiness after a temperature cycle following reassembly. The theory was that moisture entered the units because the accelerometers were not sealed during this cycle.

To provide a "superclean" accelerometer, more comprehensive processing changes were instituted as follows.

1. All components were outgassed at less than 100 micrometers.

2. Temperature cycling and magnet stabilization were performed in dry nitrogen.

3. Use of chlorothene cleaner was eliminated.

4. Use of tapwater (chlorine) was eliminated.

5. Silicone grease was eliminated from all vacuum processing.

6. Flux was eliminated.

7. The brass capacitor ring surface was cleaned with a glass brush.

8. All tape used in final assembly was outgassed or eliminated.

9. Each unit was vacuum outbaked 4 hours before final seal and backfill.

10. Each unit was filled with 75 percent dry helium and 25 percent dry nitrogen instead of 25 percent air.

11. All parts were stored in dry nitrogen.

Recycling the units through the outlined procedure did not remove the contaminant, and a pendulum remained stuck on one unit. At this point, the following options were considered.

1. To embed jewels in the capacitive pickoff ring to reduce the area touching the pendulum

2. To recycle the accelerometers through an even more stringent cleaning procedure

3. To compartmentalize the accelerometers and, thereby, to separate the electrical components from the mechanical parts

4. To change the brass pickoff plates to titanium despite the difficulty in machining titanium

5. To change the accelerometer

Based on favorable results of an investigation of the 2401 accelerometer for ASA usage, a decision was made to change accelerometers.

Gyro scale-factor asymmetry. - An error source not initially under specification control produced a significant dynamic drift rate in a rotational vibration environment. The error source was gyro scale-factor asymmetry, the difference in gyro scale-factor error between a positive and a negative input rate. Although gyro scale-factor nonlinearity error was specified at 180 pulses/min to limit the asymmetry to 360 pulses/min, the drift rate d produced for a fixed, square-wave rate of 1 deg/sec is $d = 360 \times 10^{-6} \times 1 \times 0.5 \times 3600 = 0.65$ deg/hr. Results of mission error analysis revealed that, for all input rates, a value of 200 pulses/min or less was required in the Y-axis and a value of 360 pulses/min or less was required in the X-axis and the Z-axis. Examination of a wide range of input rates, in addition to the 3 deg/sec in which scale-factor nonlinearity is normally measured, revealed the scale-factor asymmetry to be as large as 500 pulses/min. Two ASA units were determined to be unacceptable for flight because of large asymmetry readings.

The effect of noise on the current pulse used to torque the gyro caused the asymmetry. The noise originated from two sources. Synchronous noise spikes of 8 kilohertz riding on the current pulse affected the area under the current pulse as it shortened and lengthened, and deformation was also found on the trailing edge of the 64 000-pulse/sec output, which determines switching of the gyro torquer current. In the corrective design changes, the synchronous 8-kilohertz value was changed to asynchronous 8.25 kilohertz to allow the noise effects to be averaged and to derive a stable 64 kilohertz separately from the frequency countdown module. A specification of 120 pulses/min at all input rates was placed on gyro scale-factor asymmetry; however, this requirement was violated at low rates after the modifications in several cases, and a curve defining allowable asymmetry as a function of input rate was specified.

Gyro resonance. - As a result of skewed-axis vibration tests on ASA units in the 3-hertz range, a determination was made that significant drift rates could be induced for sinusoidal inputs. The error source was the H-vector spin input rectification (HVSIR). In an unperturbed condition, the gyro wheel rotates in synchronism with the stator field. If a low frequency sinusoidal angular rate is applied about the spin axis, the wheel will remain in synchronism with the stator field. If the sinusoidal rate is increased, however, the magnetic effect will not be strong enough to drive the wheel in synchronism with the stator field, and the wheel will not follow the sinusoidal stator motion. Between synchronism and asynchronism, the wheel is excited at a resonant frequency. Small angular rates at this frequency (3 hertz) about the spin axis can cause large deviations in instantaneous wheelspeed and result in gyro angular momentum. If sinusoidal inputs of the same frequency and phasing are applied simultaneously about the input and spin axes, a positive spin-axis rate will cause the angular momentum to increase momentarily for positive rates applied about the input axis and to decrease momentarily for negative rates. Float precession is greater for positive inputs, and a positive drift rate results.

For the HVSIR error to become significant, the frequencies applied to the spin and input axes must be the same, be in phase, and be at the frequency of gyro resonance. Analyses and simulations proved that the LM vehicle limit cycling did not approach this condition, and no corrective action was necessary.

Accelerometer vibration limitations. - The Bell VII accelerometer had restrictive vibration limitations because of the physical construction and the low electrical damping of the loop. The accelerometer is filled with a gas; this condition provides negligible pendulum damping. The accelerometer loop was designed to accommodate accelerations of 3g for an expected mission thrust environment of less than one g. Linear random vibration ranging from 1.0g to 1.2g root mean square, derived from the LM g^2/hertz environment with a peak at 60 hertz, caused the pendulum to hit the mechanical stops and resulted in unacceptable loss of input information.

Extensive vehicle tests using line RCS firings determined the vehicle environment to be 0.7g root mean square, and the ASA was qualified at 0.9g root mean square, a very low level. Rescaling the accelerometer to 15g was studied, but replacement of the Bell VII accelerometer with the fluid-damped 2401 accelerometer removed concern for the ASA vibration environment.

Gyro output-axis rotation effect. - During bench calibration, a large misalinement shift, although less than the specification of 130 arc-seconds, was found on several units. After an investigation, the cause of the apparent misalinement was attributed to an instability in the gyro output when rotated about the output axis (OA). Analysis and testing proved that the effect was not significant in mission performance and was not a failure precursor. The cause of the phenomenon was postulated as friction between the OA pivot and the jewel. When a gyro is rotated about the OA, gyroscopic action causes the float to precess about the input axis until the OA pivot contacts the jewel. When the pivot and the jewel are touching, the resultant friction will cause a torque to be exerted on the OA shaft. The torque appears to be directly proportional to the OA rate. Reversal of the OA rotation will move the pivot off the jewel wall and will cause contact with the jewel on the other side. The error source is rectification of OA angular motion through unequal friction effects on opposite sides of the jewel.

Fast warmup oscillation. - During vehicle testing at KSC, vehicle alarms were triggered when the ASA fast warmup circuitry was in operation. The problem was due to a noise of 13 megahertz that was placed on the vehicle 28-volt line by the ASA. A 0.1-microfarad capacitor was added to the fast-warmup-unit output to eliminate the oscillations that were traced to the characteristics of a transistor in the heater circuitry.

Coldplate connection. - Helacoil inserts having a locking feature are used in the ASA for attachment of the coldplate. Repeated mounting and dismounting caused many fractures in the insert and necessitated replacement. To correct this problem, short screws that did not engage the locking mechanism were used during vehicle testing. Full length screws were used for the final mounting of the ASA at KSC.

Gyro flexible lead. - A flexible lead failure on a nonflight gyro was attributed to weakening of the lead due to the formation of silver bromide corrosion on the lead and to a nick in the lead caused by faulty workmanship. Test results revealed that bromine from the flotation fluid, polybromotrifluoroethylene, came out of solution to combine with silver lead only above 393 K (248° F). Because the ASA operates at 322 K (120° F) and the gyro was maintained in an uncontrolled environment, the failure was attributed to poor workmanship and overheating. No evidence of silver bromide was found in dismantling other units.

Abort Electronics Assembly Development Problems

The following significant problems were encountered during the development of the AEA.

Memory cycle time. - A 4-microsecond memory cycle time was the design goal originally set in the AEA program. This time was changed to 5 microseconds after the design was proved incapable of accommodating the faster cycle time.

Memory structure. - A memory failure occurred during qualification testing because of drive lines opening in the core stack. The problem was a structural failure in a hat bracket supporting one of the memory endboards. The bracket was strengthened, and the unit subsequently passed qualification tests.

Sideplate screws. - Vibration caused loosening of several screws inside and outside the AEA. Manufacturing procedures were changed to torque all screws in a specified sequence to a designated level (68 ± 5.6 joules (6 ± 0.5 inch-pounds)). The addition of a sealing compound to the external screwheads was also necessary, although use of the compound was undesirable because of potential contamination.

Clock. - An external clock was used in the programer concept for the AGS, and this concept was carried over to the AEA to minimize vehicle EMI and synchronization problems. The AEA used a frequency of 1.024 megahertz from the vehicle instrumentation master clock. The PGS clock provides a synchronization clock output to the instrumentation clock. Results of testing revealed that activation of the primary system produced initial noise transients through instrumentation that affected the AEA memory. After evaluating and rejecting the possibility of adding a one-shot multivibrator to the AEA clock input, a free-running (18-pulse/min stability), independent

crystal oscillator was installed in the AEA to correct the problem. Problems were encountered in crystal procurement in that frequency shifts down to one-third the fundamental frequency of 1.024 megahertz were observed. These shifts were caused by lower resistance at some harmonics than at the fundamental frequency. The specification on the crystal was for a response (6 decibels down) only in the region within 25 percent of the fundamental frequency. A tank circuit was placed after the crystal to attenuate spurious frequencies.

Cable discoloration. - Several AEA Teflon-coated, shielded cables turned green and were replaced. The discoloration started at the connector end and extended up the cable. The chemically passive substance was a resin salt from the resin flux used in soldering.

Thermal discoloration. - A classic thermal discoloration (purple plague) problem was encountered in the AEA program on the transistors having a gold-to-aluminum bond. The parts were replaced with substitutes having aluminum-to-aluminum internal bonds.

Write pulse undershoot. - A memory loss problem occurred that was traced to the shape of the write pulse in the coincident current memory. The sharp fall time of the write pulse resulted in an undershoot that added to the inhibit pulse such that the state of the core could be changed. The timing circuitry was redesigned to slow the fall of the write pulse from 40 to 200 nanoseconds (1500-nanosecond pulse) and to eliminate the undershoot.

Ceramic capacitors. - Ceramic capacitors had a workmanship/design fault in that the nailhead bond that connects the external leads to the ceramic slug did not have enough surface area (0.0152 square millimeters (30 mils)) to form a good bond, and the leads, under stress, broke off at the slug. The problem was compounded by the fact that the capacitor is square; after soldering to the board, twisting to make the capacitor lie flat caused tension on the leads. The ceramic capacitors were replaced.

Sense amplifier transformers. - Six failures were encountered with one of the transformers because of lack of stress relief between the internal coil and the attaching lead. The problem was not discovered during part lot qualification testing because no stress was put on the lead until AEA installation. These parts were replaced.

Split-pin wire wrapping. - The split-pin wire wrapping technique used to connect the terminals from the multilayer boards to the matrix board had an inherent flaw. The end of the wire wrapping was anchored into the barrel or hole in the matrix board through which the multilayer board pin extended, and the pin was then wire wrapped. This pigtail penetrated the silicone rubber of the matrix board and shorted to the adjacent pin. Each AEA was rewrapped to eliminate this potential failure mode.

Nylon washers. - The nylon washers used to support screws holding the bus bars in the AEA caused a problem. Cold flow of the nylon away from the screws allowed the screws to exert normal tension on the double bus bar configuration and resulted in

shearing of the nylon insulation and short circuiting of the two bus bar layers. The nylon washers were replaced with metal washers.

Read/write memory coupling. - An intermittent memory loss problem was discovered on several AEA units because of capacitive coupling between the read pulse and the write clock through a heat sink in the mounting multilayer board. The fall time of the read clock fell sharply in 40 nanoseconds and produced a coupling into a transistor that generated the write clock. The memory problem occurred because the write clock was initiated early by the falling read clock pulse. The proposed design change to correct this problem consisted of increasing the bias on the write transistor from 1.5 to 4 milliamperes to overcome the 2-milliampere noise from the read clock. In the course of the investigation, however, another problem appeared 40 nanoseconds after the read clock cutoff. The fast fall of the read clock cut off a read driver so quickly that the back electromotive force (emf) of the stack inductance caused a transistor in the read driver to break down (30 volts applied base to emitter) under cold conditions (283 K (50° F)) in which the stack uses more current. The breakdown caused insertion of a pulse into the power system and triggering of the write pulse. To correct this problem, the read clock fall time was slowed to 150 nanoseconds, and a clamp was placed on the write clock transistor.

Multilayer board repairs. - The need for an approved rework procedure for multilayer boards to meet manufacturing schedule requirements became apparent early in the program. Haywiring was approved but was limited to five haywires per board; the restriction was later changed to seven per board.

Glass resistors and diodes. - Longitudinal cracks were found in 11 glass resistors and diodes following qualification testing. The problem was traced to low-temperature exposure (244 K (-20° F)) used to simulate unpackaged ground handling. The thickness of the conformal coating was the cause of the problem. The thicker the coating, the greater the tendency for the components to crack. The electrical characteristics of the components were unaffected. Because the lower limit of the flight environment is 273 K (32° F) and not a factor, a ground-handling restriction of 263 K (15° F) was established after testing to resolve the problem.

Corrosion. - During a 2-week period of troubleshooting on one AEA with the end plates removed and the cold rails intermittently operated, extensive internal corrosion developed because of moisture condensation. The gold flashing was penetrated, and aluminum oxide (nonconductive) and copper hydroxide (conductive) developed widely. A power supply short circuit developed because of the conductive copper hydroxide. Test procedures were changed to preclude recurrence of this problem. External AEA corrosion, aluminum oxide, was also noted in the field. The areas were cleaned and covered with a protective coating.

Overheating. - During vacuum chamber testing on the LM test article 8 vehicle at MSC, the AEA sharply overheated and had to be turned off. Extensive analysis revealed that the AEA mounting screws did not firmly compress the AEA into the room-temperature vulcanizing (RTV) resulting in a separation of the thermal path between the AEA flanges and the cold rails. Because the AEA is the only box in the LM aft equipment bay with tapered coldplate flanges, special screws, which were omitted from the test, are only required for the AEA.

Noise. - During vehicle testing, the use of several measurements on the AEA GSE connector normally unused and unconnected was impossible because of noise on the lines. The problem was traced to coupling in the matrix board. Several GSE lines, which are stepped down in voltage 10:1, were run adjacent to a 4-volt flight telemetry line. The noise, 0.6 volt, was found on the same lines for several units tested. The noise had been undiscovered previously because the GSE lines were not used, and the AEA acceptance test only included waveform pictures of flight connector outputs. Waveforms of the GSE outputs of two AEA units were made to verify that the extent of the problem was limited to the noncritical lines measured. The noisy outputs were again removed from testing.

Heat sinks. - Early in AEA production, problems encountered with burrs on metal heat sinks required that the sinks be returned to and reworked by the vendor. A filing process was not reliable in eliminating the burrs, and a grit blasting technique was adopted. The problem that burrs can create was illustrated by an intermittent memory problem, which was finally traced to a heat sink burr that penetrated the multilayer board on which it was mounted and short circuited to the first conductive layer below.

Restarts. - Vehicle-level testing revealed that the AEA was subject to frequent restarts due to power transients resulting from circuit breaker actuations. The AEA was designed to shut off at 21.5 volts with a minimum transient capability of -100 volts for 10 microseconds, or an approximate 1000 volt-microseconds. The transients experienced in the vehicle were caused by the high internal impedance of the GSE power supplies used. Flight battery transients, under the same conditions, reduced the transients by an approximate factor of 5. Results of battery analysis determined that the AEA would not be shut off in flight; however, for additional protection, the AEA was connected to a second 28-volt direct-current bus, and diodes were installed between the two buses and the AEA. Because a potential single-point failure existed if a short circuit occurred at the AEA input that would drag down the second bus supplying the PGS (i.e., the AEA circuit breaker to that bus would not throw in the required time), the second bus connection was restricted from use until after a primary guidance failure.

A restart of the AEA places the vehicle in attitude hold and shuts off the engine. The undesirable engine-shutoff feature could not be eliminated without a hardware change because a flip-flop generating the off signal comes on at random when the AEA is energized and until memory control is established. This problem was circumvented by having the crewmen augment all automatic engine-on commands with an overriding, manual engine-on command that also had other desirable features of redundancy.

Although a 1-volt line drop was added, the addition of the diodes provided another benefit in that negative transients to the AEA were eliminated and stored power could not be drained. Tests indicated that a 20-volt transient from 28 volts at the diode could be sustained for 560 microseconds before AEA shutoff.

Investigation of AEA restarts disclosed another factor potentially critical to AEA operation. The AEA normal current drain is 4 amperes, but 20 milliseconds after turn-on, when the memory is energized, an 8-ampere drain occurs for 10 milliseconds. A situation could occur, if the voltage did not rise above the AEA turn-on threshold of 23.5 volts, in which the voltage drop produced by the memory turn-on could shut the AEA off and thus result in a cycling operation that could preclude operation and destroy the memory. The requirement that the bus voltage be 26.2 volts at AEA turn-on, and following transients, was satisfied by the use of batteries. A vehicle bus alarm occurs at 26.5 volts.

Activation. - Operation of the AEA is controlled by an "off/standby/operate" switch in addition to a 28-volt circuit breaker. In the off and standby modes, a signal ground is returned to the AEA, and only a secondary AEA power supply is in operation to supply clock pulses to the ASA. Removal of the ground return places the AEA in operation. The break-before-make control switch, however, causes the AEA to go into operate momentarily between the off and standby switch positions. Contact bounce also produces the same effect. No detrimental effects were found in the use and special testing of the switch operation, although a power supply sequencing analysis indicated that the operation was undesirable for memory operation. An activation and deactivation workaround that resulted in opening the AEA circuit breaker during switch operation between off and standby was adopted.

Alinement transients. - Alinement and calibration of the AEA to the primary system is made through three AEA integrator registers that receive and store pulses representing angular increments from coupling data units in the primary system. After a discharge time of 30 minutes, capacitor switching in the coupling data units produced momentary errors as large as 0.2° to the AEA in response to angular rotations of 1.4°. Software and primary system hardware changes in the AEA were not feasible within program constraints. A 5-minute procedure for initially traversing 11.25° in each axis to close all capacitor switches was adopted for AEA IFC. Alinement of the AGS to the primary system, done instantaneously, is performed normally with crew and ground monitoring of the alinement accuracy.

Functional electronic blocks. - Functional electronic blocks, packaged combinations of thin film networks and transistors, were built for the program by the AEA vendor. The components were initially enclosed in a hollow ceramic pack; however, breakage of leads, separation during vibration, and lack of seal integrity resulted in a redesign to encapsulate the components in a molded pack. Failures of the 96 functional electronic blocks in each AEA continued to be a problem. Early failures were due to defective transistors; however, two other failure mechanisms emerged. Short circuiting of internal wires to the thin film substrate and open interconnects due to spalling were the prime failure modes. The spalling, or chipping of the thin film substrate, was related to the use of adhesive for bonding within the functional electronic block (FEB). The rigidity of the adhesive, combined with the differential coefficients of thermal expansion of the FEB elements, produced the spalling. The spalling problem was corrected by the use of a different type of adhesive. The transistor type was changed and improved inspection procedures corrected the short circuiting to the substrate.

Data Entry and Display Assembly Development Problems

The following significant problems were encountered in the development of the DEDA.

Clock. - During testing, the 128 000-pulse/sec clock from the AEA to the DEDA caused DEDA malfunctions due to transmission line effects. A 2-microsecond clock pulse from the AEA triggers a 2-microsecond one-shot multivibrator in the DEDA input circuitry. An inflection on the trailing edge of the clock pulse produced by transmission line characteristics retriggered the DEDA one-shot multivibrator. The design correction shortened the AEA clock pulse from 2 microseconds to 1 microsecond.

Electroluminescent display delamination. - Group B testing to qualify the EL part lots produced an EL failure that appeared as hemispherical chips from the edges of the display segments. The failure was due to loss of adhesion between the EL conducting film and the glass surface. Low-temperature exposure caused the separation. The EL display was tested to a temperature of 225 K (-55° F) as part of the group B testing. No delamination was seen in the qualification unit that was exposed to a temperature of 244 K (-20° F), which was well below that of the flight environment. The suspect lot was pulled, and no further corrective action was taken other than inspecting all DEDA units for similar discrepancies.

Electroluminescent display mounting. - A series of problems was encountered in mounting the EL display. A rubber gasket was initially placed over the EL display, and the display was forced against the front panel by a bracket. During vibration, the EL glass face cracked. In the second design, the EL display was bonded to a bracket that held the display away from the front panel. During qualification, the bond line between the bracket and the EL display cracked because of a difference in thermal expansion between the aluminum bracket and the Kovar of the EL display. (Kovar is necessary to match the thermal expansion of glass.) The bonding epoxy, selected because of the expansion difference, was too thin in the cracked area. In addition, the EL display short circuited because of separation of the soluthane encapsulant from the back of the EL panel, allowing salt water to reach the connection pins. The corrective action was to control the epoxy thickness bonding the EL to the mounting bracket to greater than 0.013 centimeter (0.005 inch), to place silicone rubber between the EL display and the front panel to form a gasket, to place silicone rubber on the sides and rear of the EL over the soluthane, and to remachine the front panel to eliminate any possibility of the EL display touching the panel.

Electroluminescent display. - During qualification, six EL segments failed during a 4-hour period. The cause of failure was traced to a contaminant between the primary and secondary electrodes of the segments. The electrodes are deposited in sheets. The failure mode was a series of minute thermal explosions that blasted holes in the electrodes until the line of connection between the two was broken to cause an open circuit. The contaminant originated from an epoxy mound between the centers of the two overlapping electrode sheets used to support a bridging element that supplied power to the secondary electrode. In the silk-screening process for this lot of displays, initial misplacement of the screen necessitated removal and replacement of the epoxy, which resulted in smearing and a contaminant film.

Another EL display problem encountered in qualification was darkening of the segments because of a leak in the hermetically sealed display. The leak was caused by rework that stripped RTV from a pinhole in the solder seal. When power was applied, the moisture introduced caused an electrolysis effect that allowed zinc from zinc sulfide in an internal bonder to deposit around the phosphor. Darkening was immediate. Acceptance testing and normal operation were determined to be an adequate screen for leaks in the EL display.

Switches. - The DEDA switches activated by each pushbutton are of the two-pole, double-throw type. Both contacts must close in the numeric pushbutton switches for activation; but in such functions as clear, enter, and readout, one switch activates the DEDA and the other the AEA. This configuration was chosen for ground isolation. Because the switches must throw simultaneously (within 30 milliseconds) to prevent illumination of an "operator error" light, close tolerances were necessary in manufacturing. Microswitch pairs were selected initially and adjusted after installation to throw within ±0.0063 centimeter (±0.0025 inch). The electrical actuation was then determined not to vary more than 5 milliseconds.

An anomaly during the LM-3 flight occurred when the pushbutton switch for clear operated intermittently because the AEA did not receive the discrete signal. For subsequent flights, a wiring change was made to the pushbutton switches for hold, enter, readout, and clear so that if either switch contact closed, both assemblies would receive the signal. This change introduced EMI problems, however, in that the DEDA became susceptible to coupled noise transients on the lines between the AEA and the DEDA. The 4-volt logic lines were injected with as much as 6 volts of peak-to-peak noise when various alternating-current circuit breakers were thrown in the spacecraft. The voltage drop caused by noise simulated pushbutton switch activation and caused the DEDA operator error light to illuminate. The operational procedure of clearing the DEDA after these occurrences was introduced.

Pushbutton. - Binding of the DEDA pushbutton was observed on two assemblies to the extent that the pushbuttons would remain depressed until tapped. The problem was galling of the nylon pushbuttons by the stainless steel sleeve in which they rode. To correct the problem, the sticky pushbuttons were removed, and the sides were smoothed. In addition, a force criterion of 14 newtons (50 ounces) maximum was established for the sides and corners of the pushbutton to augment the center depression requirement of 4 to 8 newtons (15 to 30 ounces).

Pushbutton leaks. - During vehicle thermal-vacuum tests at KSC, a phenomenon occurred because of leaks in the hermetically sealed DEDA pushbuttons. When the vacuum was broken, a pushbutton was depressed and then returned over a period of time. This condition was caused by pressure change: the sealed bellows assembly was evacuated during vacuum testing; after ambient conditions were regained, atmospheric pressure forced depression of the pushbutton. Because the leaks were small, pressurization of the bellows assembly was slow. Analysis and tests confirmed that this action would not take place in the mission environment of 39 985 N/m^2 (5.8 psia). The DEDA vacuum acceptance test, which included a 1-hour leak test for the hermetically sealed DEDA, was expanded to 5 hours to detect leaking pushbuttons, and all field DEDA units were vacuum screened.

Transformers. - Certain DEDA transformers in the 4-volt supply line from the AEA had reversed windings. This type transformer was used as an inductor, and the effect was to lower the phase margin of the feedback controlled loop to 4° and cause oscillations on the line because of the underdamped condition. The cause of the problem was attributed to improper workmanship in connecting the leads. The transformers were replaced. Because of the split of this power supply between the AEA and the DEDA, the phase margin of the power output was not tested in assembly.

"Galloping eights". - A faint, flickering background illumination of the digit 8 in all EL digit windows ("galloping eights") was noticed when the EL intensity was maximum in a dark room. The illumination was not noticeable under normal lighting or with lower intensity (below 115 volts to the EL windows). The method by which the DEDA display is updated by the computer caused the problem. Twice-per-second data from the displayed memory location are fed serially through the data window to the address in the proper order. The result is to produce flickering of all EL segments as the data are shifted, giving the appearance of the figure 8. The possible design correction was to blank the display during the period of AEA updating; however, this correction was not considered necessary because the illumination did not interfere with reading the DEDA, even under worst-case lighting conditions.

Abort Guidance System Software Development Problems

The following significant changes and problems were encountered in the development of AGS software.

Memory capacity. - The selection of a 4096-word memory was made with the knowledge that strong pressures would exist to expand the memory during the program. In early 1966, approximately 1 year after program inception and 3 years before flight, only 20 unassigned memory locations were available because of the requirements growth characteristic of program development. Because of skilled contractor programing and judicious selection of software functions, the mission changes were accommodated within the memory capacity.

Radar filter. - The necessity for performing state vector updates with radar information initially resulted in a simple filter effective to a range of 185 kilometers (100 nautical miles). The mission change to the coelliptic flight plan changed the accuracy requirements because of longer ranges and a reduced fuel budget. Range-rate information was added to the existing range computations, and, to accommodate CSM ranges of 741 kilometers (400 nautical miles), the radar filter was redesigned.

Design mission. - The AGS hardware is evaluated against three criteria for selloff or after a bench calibration: ASA specification values; predicted ASA performance after EPC, IFC, or lunar surface calibration (LSC); and AGS delta-V and pericynthion performance against an abort from hover design mission. By this means, the acceptability of out-of-specification ASA parameters may be determined. Maintaining a representative design mission has proved exceedingly difficult because contractual action is required to change hardware criteria and mission definitions and techniques are extremely fluid. Significant changes to each flight have demonstrated that detailed mission criteria will remain obsolete and that a worst-case design mission must be selected and fixed for hardware evaluation.

Flight director attitude indicator computations sign. - A simple sign error in the transformation matrix for driving the flight director attitude indicator was found in vehicle testing and corrected.

Direction cosine algorithm. - Interpretive computer simulations of the direction cosine algorithm determined that low angular rate limit-cycle conditions induced errors larger than the 0.2-deg/hr error budgeted for software. The drift rates were caused by the quantization selected to meet the 25-deg/sec maximum angular rate and the constraints of an 18-bit word length. The solution was to change program scaling at low rates to reduce the quantization errors. The selected scaling switchover point was 5.3 deg/sec; thus, three lower order bits were added below that rate.

Hardwired memory. - The functions assigned to the hardwired half of the AEA memory were carefully selected to be mission independent. Two hardwired memory configurations were planned; however, three became necessary. The first memory configuration was established for preproduction units at a time when the memory requirements could not be fully defined. The second configuration was to meet all requirements, but the direction cosine algorithm change previously described resulted in a third hardwired memory for flight units. The hardwired memory had 53 escape points to the erasable memory for program patching as required. Limited use was made of the escape points in generating the flight program.

External delta-V maneuver. - Orientation of the LM to a predicted, desired thrust attitude relative to a real-time local-horizon coordinate system became desirable. The capability was added to input through the DEDA down-range, cross-range, and radial velocity components to be burned; have the AGS orient the vehicle to the resultant vector; and then rotate the vehicle to maintain the vector with respect to local vertical. The V_G vector is frozen in inertial space by sensed thrust initiation. This mode also provides orbital-rate steering by using fictitious delta-V inputs that result in maintaining a fixed attitude relative to the surface.

Communication maintenance. - The necessity for maintaining the S-band communications locked on the Earth during powered descent and ascent required that the vehicle yaw angle be selectable. The equation for the attitude error about the body X-axis was changed to allow this flexibility.

Automatic exit from lunar aline. - The original implementation of lunar alinement allowed the mode to be maintained until ascent thrust was sensed, whereupon the attitude reference would go inertial. Inaccuracies due to loss of attitude pulse counts caused by the mechanism of the switchover resulted in the elimination of lunar alinement to save program steps. After the change, lunar aline was exited manually within 4 minutes of lift-off and without significant attitude reference errors because of lunar rotation.

Attitude update. - The mission capability of the AGS was taxed as the lunar landing mission became more complex. A navigation performance improvement was achieved by updating LM altitude through the DEDA during powered descent. An update between 610 and 2134 meters (2000 and 7000 feet) of altitude, based on landing radar information, significantly improved navigational accuracy, even though the accuracy of the update was ±305 meters (±1000 feet).

Insertion altitude. - The requirement that the AGS achieve a 9144-meter (30 000 foot) clear pericynthion orbit at insertion necessitated a change in the early concept of inserting at a 15 240-meter (50 000 foot) altitude. The insertion altitude was changed to 18 288 meters (60 000 feet). Because lunar landing sites could be several thousand feet below the mean lunar radius, another problem developed in achieving pericynthion. The pericynthion requirement was changed to be applicable to the landing site radius because pericynthion occurs near and behind insertion.

Lunar module state vector initialization. - A mission procedure that was adopted to improve AGS accuracy was that of inserting a canned LM state vector, representative of LM conditions after landing, into the AEA before powered descent. On landing, the LM state vector was initialized by DEDA so that early aborts on AGS would benefit from improved navigation.

Insertion targeting. - The original insertion targeting was based on a direct transfer trajectory to the CSM or on placement of the LM in a parking orbit of insertion altitude. This concept was changed to insertion target conditions of altitude, radial velocity, and horizontal velocity. These targets were revised to injection altitude, injection altitude rate, and orbit semimajor axis definition. Variable insertion targeting was later introduced to automatically change the orbit at insertion based on the CSM phase angle.

Lunar surface calibration. - The equations for lunar surface gyro calibration were initially simplified so that the inertial Y-axis was assumed to be within 10° of parallel with the lunar poles. With the adoption of inclined lunar orbits and landing sites off the lunar equator, errors were necessarily built up assuming all lunar rotation about the Y-axis. Three components of lunar rate compensation were added to replace the one required initially.

Program timing improvement. - Verification testing of an early flight program indicated that a simulation automatic time alarm triggered at the set value of 19.5 milliseconds. Because the maximum execution time allowable in a branch is 20 milliseconds, a computational segment was moved to a less critical branch.

Abort/abort-stage steering constraint. - As originally programed, presence of the abort or abort-stage discrete command was necessary for guidance steering. Because arming of the engines was produced by this action, even when RCS maneuvers were to be performed, the abort/abort-stage constraints on steering were removed.

Angle to local horizontal. - During the LM-4 flight, the crewmen noted a discrepancy between the PGS and the AGS in that the angle between the Z-axis and the local horizontal calculated by the two systems disagreed. The AGS had computed the in-plane projection of the Z-axis and the local horizontal, whereas the primary system calculated the actual angle. The AGS in-plane calculation was implemented to facilitate chart rendezvous solutions. Because the crewmen could recognize the difference, a change was not made to correct the calculation.

Apofocus and perifocus. - The desirability of supplying the crewmen with more trajectory information than originally planned became evident. A change was instituted that would provide apofocus altitude and time until perifocus to complement the available perifocus altitude.

Constant differential height maneuver. - To increase rendezvous flexibility, a change was made to enable performance of the CDH maneuver at either the first or third apsidal crossing, rather than only at the first crossing.

Out-of-plane maneuvers. - For increased mission flexibility, performance of out-of-plane maneuvers at CSI and CDH to set up in-plane rendezvous became desirable. To provide this capability, the CSI and CDH calculations were expanded.

Node after terminal phase initiate. - The direct transfer resulting from TPI was augmented by having the TPI maneuver create a node 90° down range. This maneuver allowed for performing a midcourse correction at the node to place the LM and the CSM in the same orbit plane for the remainder of the rendezvous.

The AGS/PGNCS mechanical misalinement. - Because the critical alinement of the ASA and the PGS was controlled by mechanical interfaces, no hardware adjustment capability was provided. Alinement correction provisions were included originally in the software; however, because optical and accelerometer output alinement readings confirmed the integrity of the mechanical interface, the provision was deleted to obtain the memory locations. Similarly, a rendezvous radar boresight alinement compensation provision was deleted.

Radial jerk. - To eliminate excessive vehicle maneuvers during powered ascent, a steering constraint was implemented by limiting radial jerk $\dddot{r}$ in the computations. The narrow limits imposed on $\dddot{r}$, however, reduced the capability of the LM to achieve the desired insertion conditions from a wide range of trajectory perturbations. A decision was made to allow larger off-nominal conditions to be removed when sufficient fuel was available. The $\dddot{r}$ computations were revised to make the limits on $\dddot{r}$ a function of vehicle configuration and thrust magnitude.

Simulated flight. - During a simulated lunar ascent performed as part of vehicle checkout, an out-of-plane inertial velocity of 1.5 m/sec (5 ft/sec) was recorded, although body axis velocity did not record the out-of-plane component. The problem was traced to roundoff following transformation of the compensated sensed velocity from body to inertial coordinates in the 20-millisecond computing cycle. For simulated flight testing of the AGS, an accelerometer calibration was performed to compensate for accelerometer bias and input "gravity." The compensation is added to the accelerometer output data every 20 milliseconds, and the resulting compensated velocity is transformed to inertial coordinates, rounded, and rescaled. The error buildup resulted when the compensation, because of the particular value required for this vehicle orientation and accelerometer bias, was consistently rounded down in computation periods when an accelerometer pulse was not present. The flight effects in a dynamic environment were negligible. To correct this problem, the effect of static roundoff error was calculated and included in test result evaluations.

Capability Estimate

Statistical summaries of measured AGS performance and error models for AGS evaluation are given in tables VII to X. The data were generated from ensemble

information from 18 systems for 2 years. The error models defined the AGS performance in the lunar mission after bench preinstallation calibration (PIC), EPC, IFC, and LSC. Time-stability periods used were 60 days for PIC, 18 days for EPC, and 3 days for IFC and LSC.

TABLE VII. - ABORT GUIDANCE SYSTEM ERROR MODEL I CAPABILITY ESTIMATE[a]

Error source	Axis	Unit	Mean	Gaussian 3σ	Uniform max. value
Gyro static drift rate uncorrelated	X Y Z	deg/hr	NA[b] NA NA	0.52 .53 .53	-- -- --
Gyro powered descent dynamic drift rate	X Y Z	deg/hr	NA NA NA	0.46 .30 .43	-- ±0.33 --
Gyro powered ascent dynamic drift rate	X Y Z	deg/hr	NA NA NA	0.56 .33 .52	-- ±0.37 --
Gyro coasting ascent dynamic drift rate	X Y Z	deg/hr	NA NA NA	NA NA NA	±0.07 ±.07 ±.07
Gyro drift mass unbalance (correlated)	X	deg/hr	NA	NA	NA
Gyro SA mass unbalance (uncorrelated)	X	deg/hr/g	NA	0.73	NA
Accelerometer bias, nonlinearity, and vibration-induced error[c]	X Y Z	μg	NA NA NA	190 235 233	NA NA NA
Gyro attitude scale-factor uncertainty	X Y Z	deg/deg	NA NA NA	310×10^{-6} 310 310	$\pm 94 \times 10^{-6}$ ±151 ±92
Accelerometer scale-factor error	X Y Z	g/g	48×10^{-6} 48 48	65×10^{-6} 65 65	NA NA NA
Gyro IA misalinement	X, Y Z, Y	arc-sec	NA NA	135 178	NA NA
Accelerometer IA misalinement	Y, X Z, X	arc-sec	NA NA	105 69	NA NA
Initial attitude alinement error	X Y Z	arc-min	NA NA NA	7.57 7.57 7.57	NA NA NA

[a]PIC calibration of X-gyro SA mass unbalance, gyro scale factor, and accelerometer scale factor; IFC calibration of gyro bias and accelerometer bias; PGNCS aline; abort from end of hover.

[b]NA = not applicable.

[c]Accelerometer bias, nonlinearity, and vibration-induced error are based on IFC with the RCS engines firing. With the RCS engines not firing, the X, Y, and Z bias values would reduce to 121μg, 108μg, and 106μg, respectively.

TABLE VIII. - ABORT GUIDANCE SYSTEM ERROR MODEL II CAPABILITY ESTIMATE[a]

Error source	Axis	Unit	Mean	Gaussian 3σ	Uniform max. value
Gyro static drift rate (uncorrelated)	X Y Z	deg/hr	NA NA NA	0.70 .68 .68	-- ±0.13 ±.01
Gyro powered descent dynamic drift rate	X Y Z	deg/hr	NA NA NA	0.39 .22 .38	-- ±0.33 --
Gyro powered ascent dynamic drift rate	X Y Z	deg/hr	NA NA NA	0.50 .27 .48	-- ±0.37 --
Gyro coasting ascent dynamic drift rate	X Y Z	deg/hr	NA NA NA	NA NA NA	±0.07 ±.07 ±.07
Gyro drift mass unbalance (correlated)	X	deg/hr	NA	0.61	NA
Gyro SA mass unbalance (uncorrelated)	X	deg/hr/g	NA	0.57	NA
Accelerometer bias, nonlinearity, and vibration-induced error[b]	X Y Z	μg	NA NA NA	190 235 233	NA NA NA
Gyro attitude scale-factor uncertainty	X Y Z	deg/deg	NA NA NA	310×10^{-6} 310 310	$\pm 94 \times 10^{-6}$ ±151 ±92
Accelerometer scale-factor error	X Y Z	g/g	48×10^{-6} 48 48	65×10^{-6} 65 65	NA NA NA
Gyro IA misalinement	X, Y Z, Y	arc-sec	NA NA	135 178	NA NA
Accelerometer IA misalinement	Y, X Z, X	arc-sec	NA NA	105 69	NA NA
Initial attitude alinement error	X Y Z	arc-min	NA NA NA	7.25 7.25 7.25	NA NA NA

[a]PIC calibration of X-gyro SA mass unbalance, gyro scale factor, and accelerometer scale factor; EPC calibration of gyro bias; IFC calibration of accelerometer bias; PGNCS aline; abort from end of hover.

[b]The accelerometer bias, nonlinearity, and vibration-induced error are based on IFC with the RCS engines firing. With the RCS engines not firing, the X, Y, and Z error magnitudes would reduce to 121μg, 108μg, and 106μg, respectively.

TABLE IX. - ABORT GUIDANCE SYSTEM ERROR MODEL III CAPABILITY ESTIMATE[a]

Error source	Axis	Unit	Mean	Gaussian 3σ	Uniform max. value
Gyro static drift rate (uncorrelated)	X Y Z	deg/hr	NA NA NA	0.43 .42 .42	NA NA NA
Gyro powered descent dynamic drift rate	X Y Z	deg/hr	NA NA NA	NA NA NA	NA NA NA
Gyro powered ascent dynamic drift rate	X Y Z	deg/hr	NA NA NA	0.50 .27 .48	0 ±0.37 0
Gyro coasting ascent dynamic drift rate	X Y Z	deg/hr	NA NA NA	NA NA NA	±0.07 ±.07 ±.07
Gyro drift mass unbalance (correlated)	X	deg/hr	NA	0.73	NA
Gyro SA mass unbalance (uncorrelated)	X	deg/hr/g	NA	NA	NA
Accelerometer bias, nonlinearity, and vibration-induced error[b]	X Y Z	μg	NA NA NA	219 259 257	NA NA NA
Gyro attitude scale-factor uncertainty	X Y Z	deg/deg	NA NA NA	310×10^{-6} 310 310	$\pm 94 \times 10^{-6}$ ±151 ±92
Accelerometer scale-factor error	X Y Z	g/g	48×10^{-6} 48 48	65×10^{-6} 65 65	NA NA NA
Gyro IA misalinement	X, Y Z, Y	arc-sec	NA NA	135 178	NA NA
Accelerometer IA misalinement	Y, X Z, X	arc-sec	NA NA	105 69	NA NA
Initial attitude alinement error	X Y Z	arc-min	NA NA NA	7.57 7.57 7.57	NA NA NA

[a]PIC calibration of X-gyro SA mass unbalance, gyro scale factor, and accelerometer scale factor; LSC calibration of gyro bias; IFC calibration of accelerometer bias; PGNCS aline; abort from lunar surface.

[b]The accelerometer bias, nonlinearity, and vibration-induced error are based on IFC with the RCS engines firing. With the RCS engines not firing, the X, Y, and Z error values would reduce to 128μg, 118μg, and 116μg, respectively.

TABLE X. - ABORT GUIDANCE SYSTEM ERROR MODEL IV CAPABILITY ESTIMATE[a]

Error source	Axis	Unit	Mean	Gaussian 3σ	Uniform max. value
Gyro static drift rate (uncorrelated)	X Y Z	deg/hr	NA NA NA	0.70 .68 .68	-- ±0.13 ±.01
Gyro powered descent dynamic drift rate	X Y Z	deg/hr	NA NA NA	0.39 .22 .38	-- ±0.33 --
Gyro powered ascent dynamic drift rate	X Y Z	deg/hr	NA NA NA	0.50 .27 .48	-- ±0.37 --
Gyro coasting ascent dynamic drift rate	X Y Z	deg/hr	NA NA NA	NA NA NA	±0.07 ±.07 ±.07
Gyro drift mass unbalance (correlated)	X	deg/hr	NA	0.61	NA
Gyro SA mass unbalance (uncorrelated)	X	deg/hr/g	NA	0.57	NA
Accelerometer bias, nonlinearity, and vibration-induced error	X Y Z	μg	NA NA NA	163 163 163	NA NA NA
Gyro attitude scale-factor uncertainty	X Y Z	deg/deg	NA NA NA	310×10^{-6} 310 310	$\pm 94 \times 10^{-6}$ ±151 ±92
Accelerometer scale-factor error	X Y Z	g/g	48×10^{-6} 48 48	65×10^{-6} 65 65	NA NA NA
Gyro IA misalinement	X, Y Z, Y	arc-sec	NA NA	135 178	NA NA
Accelerometer IA misalinement	Y, X Z, X	arc-sec	NA NA	105 69	NA NA
Initial attitude alinement error	X Y Z	arc-min	NA NA NA	7.57 7.57 7.57	NA NA NA

[a]PIC calibration of X-gyro SA mass unbalance, gyro scale factor, accelerometer scale factor, and accelerometer bias; EPC calibration of gyro bias; PGNCS aline; abort from end of hover.

Flight Performance and Anomalies

The overall flight performance of the AGS during the first three LM missions was good except for minor hardware malfunctions that did not interfere with mission operations. Excellent inertial performance exceeded specification and capability estimate bounds. The detailed test objectives for the first three flights were as follows.

1. AGS in-flight calibration and performance (detailed test objective (DTO) P12.2)

2. AGS/control electronics system (CES) attitude/translation control, unstaged LM (DTO P12.3)

3. AGS delta-V capability using the descent propulsion system (DTO P12.4)

4. AGS performance in the flight environment (DTO S12.6)

5. AGS/CES attitude/translation control, staged LM (DTO S12.8)

6. Unmanned, AGS-controlled ascent propulsion system burn (DTO S12.9)

7. LM AGS rendezvous evaluation (DTO S12.10)

8. PGNCS/AGS monitor lunar orbit (DTO P20.82)

All detailed test objectives were met after the AGS had been flown.

The LM-3 flight (Apollo 9 mission). - The first flight test of the AGS was during the Apollo 9 mission (LM-3 flight). The AGS was operational throughout the mission and controlled a descent propulsion burn. The data recorded during the AGS calibrations are given in table XI.

TABLE XI. - FINAL PIC, FINAL EPC, AND IFC DATA OF THE AGS

Inertial instrument	Final PIC	Final EPC	IFC		
			1	2	3
Gyros					
X, deg/hr	-0.27	-0.33	-0.21	-0.07	-0.19
Y, deg/hr	-.47	-.56	-.36	-.28	-.13
Z, deg/hr	-.06	.16	.2	0	.01
Accelerometers					
X, μg	124	--	0	0	0
Y, μg	45	--	0	0	0
Z, μg	185	--	380	380	380

The AGS performance and interface specification value for gyro-fixed drift after IFC is 0.6 deg/hr. The results of the in-flight accelerometer calibration were below the DEDA quantization level for Earth orbit, 380μg. The performance and interface specification requirement was 290μg after an IFC. The flight test results, in a dynamic environment, were well within the specified value, meeting DTO P12.2 requirements. Data recorded during the in-flight determination of gyro and accelerometer bias in free flight are given in table XII. The values were well within specification and satisfied the objectives of DTO S12.6. The PGNCS/AGS alinement accuracy (coupling data unit (CDU) and AEA angular differences) for three alinements is given in table XIII, which also demonstrates the performance of DTO S12.6. The alinement accuracy specification was 0.067°

TABLE XII. - IN-FLIGHT DETERMINATION OF GYRO AND ACCELEROMETER BIAS IN FREE FLIGHT

Gyro axis	Gyro drift relation to the PGNCS, deg/hr	In-flight accelerometer bias, μg
X	0.03 ± 0.12	26.8
Y	-.14 ± .12	-43.0
Z	.10 ± .12	-53.8

TABLE XIII. - ALINEMENT ACCURACIES OF THE PGNCS DURING THE APOLLO 9 MISSION

Axis	Alinement, deg		
	1	2	3
X	0	0.005	0.04
Y	0.02	.002	.02
Z	-.003	.02	.01

The performance of DTO P12.4 was demonstrated by the AGS control of the LM phasing burn. The V_G residual in the PGNCS after the burn was 0.42 m/sec (1.38 ft/sec). The same residual for the AGS was 0.3 m/sec (1.0 ft/sec). A comparison of the V_G magnitudes for all burns is given in table XIV.

TABLE XIV. - A COMPARISON OF THE

V_G MAGNITUDES FOR ALL BURNS

Burn	Velocity, m/sec (ft/sec)	
	AGS	PGNCS
Docked	1.7 (5.5)	1.29 (4.24)
Phasing	.3 (1.0)	.42 (1.38)
Insertion	.3 (1.0)	.21 (.70)
CSI	.4 (1.5)	.36 (1.18)

The performance of DTO S12.10 was accomplished partly by the AGS guidance solutions for the rendezvous maneuver. A comparison of the AGS computed V_G with that calculated by the ground for the rendezvous maneuvers (table XV) showed a close correlation.

TABLE XV. - A COMPARISON OF THE RENDEZVOUS MANEUVER

VELOCITIES AS COMPUTED BY THE AGS AND THE GROUND

Rendezvous maneuver	Velocity, m/sec (ft/sec)	
	AGS	Ground solution
CSI V_G	26 (86)	25 (81)
CDH V_G	13 (42)	12.5 (41.1)
TPI V_G	6.5 (21)	6.8 (22.2)

The requirement of DTO S12.3 was satisfied by vehicle manual control during the LM-3 mission. The AGS performed properly in providing attitude-hold capability in conjunction with the CES.

Two anomalies occurred during the Apollo 9 mission. At AGS turn-on preparatory to the rendezvous phase, the AGS C&W light illuminated and remained on for the duration of the AGS active phase. The light could be activated by an overtemperature ASA, by out-of-specification ASA power supply voltages, and by an AEA test mode failure. Because the AEA self-test readout indicated that the computer was operating

properly and that the ASA was at the proper temperature (322 K (120° F)) and a good IFC indicated that the ASA power supplies were operating properly, the mission was continued. Subsequent AGS performance indicated that the decision was correct and that the failure was not integral to the ASA. Possible causes of the failure were an open line from one of three ASA power supply voltages to instrumentation, including opening a 339 K (150° F) thermistor in the 12-volt line for overtemperature warning; a short-circuited test-mode-fail transistor in the AEA; or several instrumentation failures. The exact cause of the operator error light was not determined but was ascribed to an instrumentation failure.

The second anomaly was reported by the crewmen after the mission. Frequently during the mission, the DEDA operator error light would illuminate following a clearing operation in the readout mode. Several depressions of the pushbutton for clear were required to extinguish the light. The problem was traced by downlink information to failure of the AEA to get the discrete signal for clear. The pushbutton for clear activates two independent microswitches adjusted to 5 milliseconds actuation, which supply the discrete to the AEA and the DEDA. If the AEA and the DEDA do not simultaneously receive the discrete signal within 30 milliseconds, an operator error light results. The failure was ascribed to an intermittent switch operation or a mechanical shift in the switch that caused an activation timing error. Similarly, a previous one-time anomaly in pushbutton switch activation for clear during ground testing had been closed as failure to fully depress the pushbutton.

The corrective action was to rewire the pushbutton switches supplying both the AEA and the DEDA. The pushbutton switches for clear, enter, readout, and hold were wired so that closure of either switch would supply the discrete signal to both the AEA and the DEDA. The DEDA acceptance test was changed to perform pushbutton switch activation in six positions and during low-level vibration.

The LM-4 flight (Apollo 10 mission). - During the Apollo 10 mission (LM-4 flight), the AGS controlled undocking, staging, ascent propulsion burn to depletion, and wide and narrow dead band attitude-control tests. This mission, in conjunction with the Apollo 9 mission, exercised all AGS functions except orbital insertion guidance and lunar surface operations. Three AGS alinements to the PGNCS that resulted in CDU/AEA angular differences within the 0.067° specification are given in table XVI.

TABLE XVI. - ALINEMENT ACCURACIES OF THE PGNCS DURING THE APOLLO 10 MISSION

Axis	Alinement, deg		
	1	2	3
X	0.038	0.021	0.03
Y	.028	.005	.01
Z	.027	.023	.06

A calibration of gyro and accelerometer biases was not performed during the mission as scheduled. The calculated performance information given in table XVII supports DTO S12.6. The accelerometer bias was taken during a 20-minute period across the phasing burn.

TABLE XVII. - GYRO AND ACCELEROMETER CALIBRATIONS

Bias	X	Y	Z
Accelerometer bias, μg . . .	-56	6	-11
Gyro bias, deg/hr	-.14	-.02	-.16

Data from four state vector transfers from the PGNCS to the AGS provided the following accuracies in support of DTO S12.6: 457 meters (1500 feet), 0.09 m/sec (0.3 ft/sec); 183 meters (600 feet), 0.2 m/sec (0.6 ft/sec); 152.5 meters (500 feet), 0.4 m/sec (1.3 ft/sec); and 152.5 meters (500 feet), 0.09 m/sec (0.3 ft/sec). The AGS burn residuals in comparison with those of the PGNCS (table XVIII) indicated close agreement in support of DTO P20.82. The AGS targeted delta-V for the TPI maneuvers was 7.39 m/sec (24.25 ft/sec). The PGNCS target was 7.3 m/sec (24.1 ft/sec).

TABLE XVIII. - A COMPARISON OF AGS AND PGNCS

BURN RESIDUALS

Burn	Velocity, m/sec (ft/sec)	
	AGS	PGNCS
Phasing burn	0.6 (2)	0.3 (1)
Insertion	.33 (1.1)	.5 (1.7)
CDH	.06 (.21)	.03 (.1)
TPI	.1 (.4)	.03 (.1)

The burn to completion on the AGS satisfied DTO S12.9. A burn of 1164 m/sec (3820 ft/sec) was performed. The largest AGS attitude error was 0.1°. The AGS burn residual was 232 m/sec (762 ft/sec). The PGNCS burn residual was 233 m/sec (765 ft/sec). A series of AGS wide and narrow dead band attitude-hold tests was performed after the burn to depletion to satisfy DTO S12.8.

Two anomalies occurred during the LM-4 flight. After undocking, the crewmen noted a discrepancy of 20° between the AGS angle of the vehicle Z-axis with respect to local horizontal and the angle displayed by the PGNCS. This discrepancy was caused by a difference in the way the angle was calculated in the two systems. The actual Z-axis was used for the PGNCS calculation, whereas a projection of the Z-axis in the orbital plane was used for the AGS calculation. The AGS calculation had been changed to the in-plane projection to facilitate use of chart solutions. The second anomaly occurred at staging. A large attitude transient occurred at staging because of the AGS mode of control selected. The Z-axis steering, which points the LM Z-axis at the CSM, had been selected previously. When the system went into the automatic mode near staging in wide dead band, the vehicle reoriented to point the Z-axis at the CSM. Because a rate limit is not imposed in wide dead band, a rapid attitude excursion resulted.

The LM-5 (Apollo 11 mission) lunar landing. - No active AGS burns were performed on the Apollo 11 mission (LM-5 flight); however, AGS burn solutions were obtained, and AGS solutions and burn residuals were compared with those of the PGNCS. The accuracies of five AGS alinements to the PGNCS are given in table XIX. Gyro-drift performance data (table XX) were obtained by one IFC and two lunar surface calibrations performed during the mission. The results were well within specification values and supported DTO 12.2. A graph of the gyro performance history is given in figure 4.

TABLE XIX. - ALINEMENT ACCURACIES OF

THE PGNCS DURING THE APOLLO 11 MISSION

Axis	Alinement, deg				
	1	2	3	4	5
X	0.003	-0.005	0.02	-0.002	-0.003
Y	.004	.003	-.006	-.001	.005
Z	0	.01	.002	0	.003

TABLE XX. - GYRO-DRIFT PERFORMANCE DATA

Calibration	Drift performance, deg/hr		
	X	Y	Z
PIC (June 2, 1969)	0.27	0.03	0.41
Final EPC (June 28, 1969)	.1	-.13	.35
IFC (July 20, 1969)	.33	-.07	.38
LSC (July 20, 1969)	.34	-.08	.47
LSC (July 21, 1969)	.41	-.04	.5

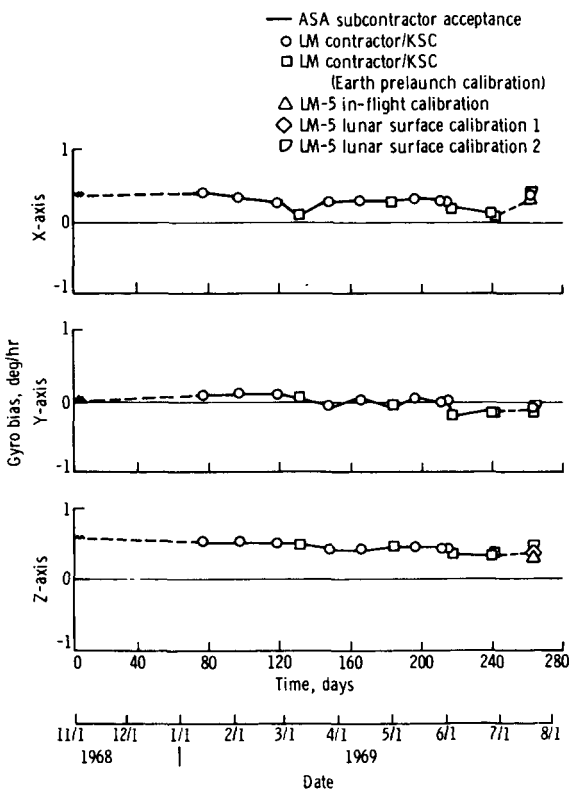

Figure 4. - Gyro bias history.

The accelerometer bias in free flight is given in table XXI. The results were well within specification values, supporting DTO 12.2. A graph of accelerometer performance history is given in figure 5.

The AGS computation of the TPI burn was 7.3 m/sec (24 ft/sec); the PGNCS solution was 7.6 m/sec (25.1 ft/sec). The AGS-computed CDH maneuver was 6.17 m/sec (20.25 ft/sec) as compared to a pad load of 6 m/sec (20 ft/sec). The AGS CSI solution was 15.4 m/sec (50.7 ft/sec) compared to a nominal 15.6 m/sec (51.5 ft/sec). The AGS orbital parameters after insertion were a 17.6- by 86.3-kilometer (9.5 by 46.6 nautical mile) orbit; PGNCS had a 17.6- by 87.6-kilometer (9.5 by 47.3 nautical mile) orbit; and the Manned Space Flight Network had a 17.6- by 89.1-kilometer (9.5 by 48.1 nautical mile) orbit. These data support DTO S12.10 and DTO P20.82.

TABLE XXI. - ACCELEROMETER BIAS IN FREE FLIGHT

Calibration	Accelerometer bias, μg		
	X	Y	Z
PIC (June 2, 1969)	1	-17	-66
Free flight (July 20, 1969)	-60	-20	-20

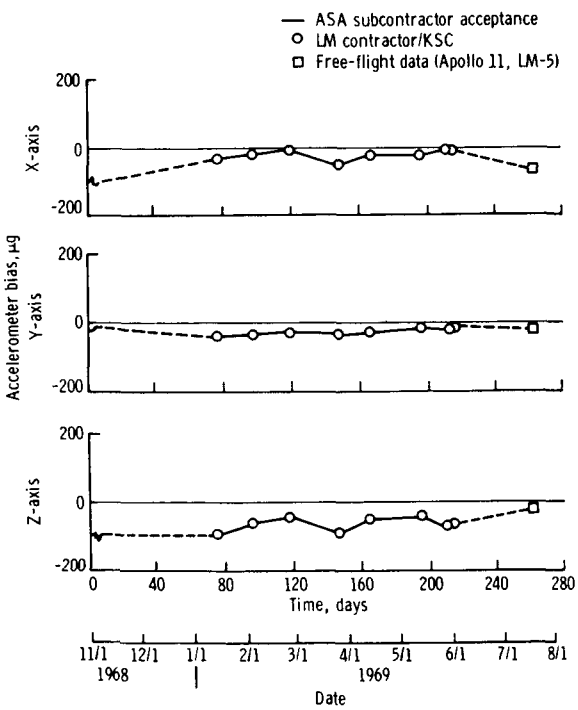

Figure 5. - Accelerometer bias history.

The AGS burn residuals compared with those of the PGNCS are given in table XXII. The AGS delta-V_Y out-of-plane error at orbital insertion was caused by a 0.087° data error in azimuth supplied to the AGS on the lunar surface. The AGS CDH residuals were 0.06, -0.06, and -0.09 m/sec (0.2, -0.2, and -0.3 ft/sec). The burn residuals support DTO S12.6.

One AGS anomaly occurred during the flight. At turn-on, one of the DEDA EL segments would not illuminate. The segment in the upper left of the middle data digit prevented the crewmen from distinguishing between a 3 and a 9. Research into component failure histories and testing did not disclose any precursor for the failure. The possibility of a pinhole leak, a delamination, or an electrode burnout was examined and discarded. The failure was ascribed to a part failure or a broken wire in the segment driver circuit. The usage, population, and history of the parts indicated that the failure was an isolated case. The only corrective action taken was to turn the EL segments to full intensity briefly during the latter portion of the checkout flow at KSC.

TABLE XXII. - A COMPARISON OF BURN RESIDUALS

Burn	Residual velocity, m/sec (ft/sec)	
	AGS	PGNCS
Descent orbit insertion		
Delta-V_X	-0.03 (-0.1)	0.03 (0.1)
Delta-V_Y	-.06 (-.2)	.1 (.4)
Delta-V_Z	-.21 (-.7)	.03 (.1)
Orbit insertion		
Delta-V_X	-0.03 (-0.1)	0.03 (0.1)
Delta-V_Y	2.7 (8.9)	.03 (.1)
Delta-V_Z	--	.1 (.5)
CSI		
Delta-V_X	0.1 (0.4)	-0.06 (-0.2)
Delta-V_Y	.3 (.9)	.21 (.7)
Delta-V_Z	.09 (.3)	-.03 (-.1)

PROGRAM OBSERVATIONS

Schedule

The development of the AGS strapped-down guidance system was scheduled for completion 1 year after project initiation. Optimistically, the first preproduction units were originally scheduled for delivery in the fall of 1965 following contractual agreement in October 1964 and program definition completion in January 1965. Some interface changes, however, were made as late as May 1965. The first unit was delivered in August 1966, although various design changes and recycling followed. In the development of a similar system, allowance of 18 months is not unrealistic.

Thermal-Vacuum Acceptance

During the AGS program, thermal-vacuum testing screened as many failures as vibration testing. Both environments should be used in assembly acceptance testing, beginning preferably with vibration so that weaknesses found by vibration will be evident during thermal-vacuum testing.

Compatibility Testing

The initial AGS deliveries were made on systems rather than on individual assemblies. After the normal acceptance test was performed on each assembly, special tests were performed with the units connected. When confidence was gained in the interface performance, the compatibility test was dropped. No significant problems were disclosed by compatibility testing. Compatibility testing could be performed as part of qualification or design-proof testing and eliminated from acceptance testing.

Dual Source Procurement

The procurement of critical parts from two sources was questioned during the initial phases of the AGS program because of the cost factor. However, numerous experiences in the program demonstrated the necessity of having an immediate alternate source of qualified parts to maintain a schedule-oriented program.

Assembly Reliability

The subcontractor satisfied the reliability goal specified for each assembly by performing the most extensive part lot screening tests (i.e., R_1-level parts that are sample tested to destruction, 100-percent environmental tested, etc.) on the most numerous parts in the assembly or on those with least usage history. Those familiar parts used in small numbers on certain cases, although meeting military standard and program requirements, were only 100-percent electrically tested and 100-percent burned in (R_8-level parts). An element of risk in this procedure was that defective parts might be introduced and result in expensive replacement. The setting of a reliability number for paper analysis should be replaced by a more stringent minimum part lot acceptance test.

Transient Protection

To prevent restarting, a 28-volt input dropout protection of a minimum of 1 second should be provided for each assembly of an inertial guidance system. Even with flight batteries of low internal impedance and excellent response characteristics, the protection was needed for vehicle operation with ground power supplies. The cutoff voltage should also be set as low as possible, preferably at 18 volts or below. A diode in the 28-volt line offered protection from negative transients and thus prevented loss of stored energy and increased time to turnoff after a power drop. The benefits from a

diode greatly exceeded the detrimental effect of the 1-volt line drop it produced. The computer software functions and the computer electrical design for startup power sequencing should include the requirement to accommodate immediate and automatic mission continuation after a power loss that causes a computer restart.

Software Development

The time required for a major software change, including verification, could be as long as 9 months for a full memory that required complete recoding. A longer time was required for a hardware change.

Memory Functions

The memory constraints of the AEA coupled with the expanding mission requirements necessitated the exclusion of many desirable software capabilities so that AGS rendezvous with the CSM could be retained. The provision for in-flight dumping of the AEA memory was excluded, as was an in-flight loading capability. Both these functions are highly desirable for future programs. Where weight requirements are not stringent, provision for an auxiliary memory should be included even though memory requirements at the time of hardware definition are marginal.

Scale-Factor Asymmetry

For future strapped-down systems, a computer provision for separate scale-factor compensations for positive and negative rotations in each gyro channel should be provided. The rectification error caused by scale-factor asymmetry in a dynamic environment would then be largely eliminated.

Electroluminescent Display

The failure of an EL display hermetic seal and the resultant introduction of moisture will produce darkening of the entire multidigit display within an hour. Future designs should compartmentalize each digit so that only one will be lost if a leak occurs.

Pushbuttons

The DEDA pushbutton design allowed the nylon caps to rub against the stainless steel sleeve. In future designs, the pushbutton should be attached to the activation shaft to prevent the cap from touching the sides of the housing.

Pushbutton Switches

The DEDA pushbutton switches are dependent on mechanical tolerances to produce the simultaneous activation of two switches within a 30-millisecond time tolerance. A

single switch, or preferably a redundant switch operation, should be used in future designs for pushbutton switches.

Environmental Testing

The effect of moisture on the assembly and the resulting corrosion could not be determined adequately if heat was maintained on the assembly during the test. Salt spray and temperature/humidity environments should be performed with the unit operative as well as inoperative.

Ground-Support-Equipment Heaters

A single heating control subassembly was used in the GSE heaters for both flight and ground temperature maintenance. Although heater life is 10 000 hours, the inoperative ASA was maintained at a temperature of 289 K (60° F) and no failures occurred. The necessity to feed power into the ASA GSE connector for ground operations would result in powering the vehicle bus if the ASA circuit breaker was left open. A better design would incorporate separate GSE heaters to maintain inertial instrument temperatures during inoperative periods.

Abort Sensor Assembly Mission Acceptance

Three levels of criteria were used for ASA selloff and evaluation after a bench calibration. The first level was comparison with specification values; the second was calculation of the stability of the bias terms after EPC, IFC, or LSC; and the third was determination of the mission delta-V and pericynthion performance. Maintaining a current mission definition contractually was difficult in the extreme. To use the third criterion for waiver evaluation, the only feasible procedure was to select a representative mission and not attempt to follow the fluctuations of mission planning.

Abort Sensor Assembly

After six production units of the inertial sensor assembly have been field tested to obtain ensemble data, the specification should be reevaluated and adjusted as necessary to make it conform to the capability of the system. By this means, the specification could be more useful in detecting unusual performance and incipient reliability problems.

Gyro Fluid

The mass unbalance shift effects ascribed to two-cut gyro fluid stratification in the ASA indicated that the use of a single-cut flotation fluid was preferable for future programs.

Gyro Resonant Frequency

To preclude significant induced drift rates caused by HVSIR errors, the frequencies applied to the gyro spin and input axes by vehicle limit cycling and their phase relationships should be compared with the gyro resonant frequency early in the design definition phase of a future program.

Engineering Model

Because of schedule constraints, the AGS program did not include the use of an engineering model for design evaluation before committing to production. Many manufacturing and circuit design problems could have been corrected early if budgetary and schedule constraints had permitted an engineering evaluation model.

Assembly Cabling

Because the LM spacecraft wiring was frozen early by rack mounting connectors for the subassemblies, pigtail cables were extended from the AEA. An alternative configuration that would have simplified the AEA design would have been to box mount the connectors and mate the spacecraft connectors to each unit.

Vibration Transmissibility

A vibration transmissibility of 10 was initially specified for all AGS assemblies. The AEA design required that the transmissibility be opened to 20, which was done with no adverse effects as proven by qualification. The use of 10-layer multilayer boards at this transmissibility factor was therefore also verified.

Split-Pin Wire Wrapping

Anchoring one end of the wire wrap in the barrel produced short circuiting to the next pin in the AEA. Future procedures should be corrected, as were those of the AEA, to eliminate pigtails on both ends of the wire wrap.

Program Incentives

The use of fee incentives on completion of qualification testing and deliveries of blocks of initial assemblies was helpful in maintaining and improving schedules for the AGS program.

Capability Retention

The staffing of capable subcontractor personnel at a minimum cost for failure closeout and repair following delivery of the last unit was a significant problem because unless desired individuals were maintained full time on the AGS program, they were

reassigned to other programs and might not be recalled in an acceptable time period. A possible solution is to require, contractually, at the inception of a major and significant program, that key individuals be made available on 2 weeks notice from production completion throughout the flight program.

Subcontractor Test Participation

The initial integration of the AGS with the LM presented many problems related to vehicle checkout. The participation of the subcontractor would have been valuable during the resolution of these problems. A review by the subcontractor of vehicle checkout procedures and onsite support during house spacecraft integration and the test of the first two flight vehicles would be beneficial in future programs; such a review would result in time savings that would outweigh the attendant costs.

Program Control

To ensure effective control of the technical and cost aspects of a subcontract by MSC subsystem personnel, the vendor change notices originated by the prime contractor to the subcontractor should be reviewed by MSC, preferably before implementation. Cost negotiations with the prime contractor for MSC-directed changes should also include subsystem technical personnel participation to ensure that the scope and the content of the change are properly defined in the negotiation.

Earth-Orbit Software Programs

The requirement to support both Earth-orbit and lunar missions resulted in a decision to supply one set of equations for both missions and to use rescaling to accommodate both environments. For Earth missions, rescaling by a factor of 4 was used without significant performance degradation. This approach, besides the advantage of economy, offered verification of the lunar mission equations in Earth orbit. In addition, flexibility was gained to convert a scheduled lunar mission to an Earth-orbit mission during flight through the use of DEDA changes to selected constants.

Test Programs

The prime contractor was responsible for AGS test and checkout programs, although the flight software was supplied as Government-furnished equipment. The prime contractor was required, however, to supply all test programs to the software vendor for verification. In this manner, effective testing of the special programs was obtained to avert test delays and to ensure the integrity of test results.

Mission Performance Analysis

Performance analyses indicating adequate delta-V margin performed early in a program should be biased to allow for vehicle weight growth and the resultant reduction in available delta-V.

Gyro Rundown Time

The use of gyro rundown time as a reliability indicator was complicated in the ASA because the generated back emf caused all three gyros to run down in approximately the same time. Future designs should provide for decoupling the three gyro wheels.

Program Evaluation Reporting Technique

The use of the program evaluation reporting technique (PERT) was not significantly valuable in the AGS program. By the time the subcontractor PERT was incorporated into the prime contractor PERT and transmitted to MSC, the data were out of date. The usefulness of the PERT remained at the subcontractor facility, where it served as a program plan and noted existing constraints and requirements.

Inertial Package Alinement

A recommended addition to future strapped-down packages is an optics cube for alinement determination. The preinstallation ASA mounting-base alinement was determined by optically shooting a fixture mounted in place of the ASA against a fixture mounted on the vehicle navigation base and against a fixture mounted in place of the PGS inertial measurement unit. After installation, the mechanical alinement was obtained by gravity leveling the primary gimbaled system and by comparing the CDU readings with the ASA accelerometer outputs. The tolerance was 4 arc-minutes. This procedure was adequate, but the capability for direct optical sightings should be provided for future systems.

Backup Guidance Definition

The crew task and training load for operating a backup guidance system that is different from the PGS was not fully appreciated at the inception of the AGS program. The simple operation originally envisioned became more and more complex as the mission profile and the AGS software were defined. The DEDA addresses could not correspond numerically to similar PGS addresses, where applicable, because limited memory capacity dictated that the memory locations be assigned according to judicious programing rather than according to compatibility with the PGNCS. Every consideration in future hardware definition should be given to placing redundancy in the primary system rather than incorporating a separate and different backup guidance system.

Nailhead Bond Capacitors

Nailhead bond capacitors should be eliminated from future designs because of limited contact area between the lead and the slug. If used, 100-percent environmental testing and X-raying should be performed on each lot to detect marginal bonds.

Flight Connector Integrity

A paramount original program objective was to maintain flight connections, once made. This objective resulted in a 120-day stability requirement on ASA inertial parameters because it was envisioned that no bench calibration could be made after beginning vehicle testing at KSC. In practice, the elimination of bench calibrations at KSC was not realistic because stability must be closely observed, selection of flight compensation constants must be made, and the ASA can be bench calibrated during periods of as many as 80 days when it is not required in the vehicle for checkout. During the testing of the vehicle at KSC, the ASA was calibrated three times at maximum intervals of 30 days.

Work Packages

The use of the work package concept for program control at the subcontractor level was very effective. The tracking of work units accomplished, compared to man-hours budgeted and actual man-hours expended, provided great insight into both schedule and cost forecasts. This control procedure is highly recommended for future programs.

Elapsed-Time Indicators and "G" Balls

Neither elapsed-time indicators nor "G" balls were reliable in the AGS program. The timekeeping was erratic, and the "G" balls, set at 15g, were often sprung after hardware shipment or transportation from room to room. Recording accelerometers should be used on handling and shipping devices. Proper packaging and handling was found to be the only viable means of assuring hardware protection during transportation.

Checkout Meetings

Organized monthly checkout meetings at KSC were extremely beneficial in the AGS program. Common discussion of test requirements, criteria, schedule, procedures, and problems among prime contractor, subcontractor, MSC, and KSC personnel was important in ensuring the integrity of the flight vehicle.

Computer Startup Sequence

In designing a computer startup sequence, particular attention should be given to the sequence of current requirements. In the design of the AEA, the memory was turned on 20 milliseconds after the logic to ensure memory integrity. The normal 4-ampere load was increased to an 8-ampere mandatory load at memory activation.

It was feasible for the attendant line drop for memory activation to lower the input voltage below the computer cutoff level; this practice resulted in computer on/off cycling for low bus voltage levels at computer turn-on.

Operator Error Lights

All operator error and warning lights should be placed on GSE outputs or telemetry to time correlate the occurrence of failure indications for anomaly resolution.

CONCLUDING REMARKS

The feasibility of a strapped-down guidance system of inertial quality has been demonstrated in the lunar module program by the abort guidance system. The number of problems encountered were not inordinate for a new development of this type, and successful resolution of the problems resulted in remarkable performance during the lunar landing missions. Confidence has therefore been established in the application of strapped-down guidance systems for future space programs.

Lyndon B. Johnson Space Center
National Aeronautics and Space Administration
Houston, Texas, October 18, 1974
976-10-41-01-72

NASA-Langley, 1975 S-424